Materials Today Chemistry 26 (2022) 101144

Contents lists available at ScienceDirect

Materials Today Chemistry

journal homepage: www.journals.elsevier.com/materials-today-chemistry/

Nonordered dendritic mesoporous silica nanoparticles as promising platforms for advanced methods of diagnosis and therapies

S. Malekmohammadi [a], R.U.R. Mohammed [b], H. Samadian [c], A. Zarebkohan [d, e], A. García-Fernández [f, g, h], G.R. Kokil [i], F. Sharifi [j], J. Esmaeili [k], M. Bhia [l], M. Razavi [m, *], M. Bodaghi [n, **], T. Kumeria [i, ***], R. Martínez-Máñez [f, g, h, ****]

[a] School of Materials, University of Manchester, Engineering Building A, MECD, Manchester, UK
[b] Biomedical Engineering, University of Nebraska Lincoln, Nebraska, Lincoln, USA
[c] Research Center for Molecular Medicine, Hamadan University of Medical Sciences, Hamadan, Iran
[d] Department of Medical Nanotechnology, Faculty of Advanced Medical Science, Tabriz University of Medical Sciences, Tabriz, Iran
[e] Nanomedicine Research Association (NRA), Universal Scientific Education and Research Network (USERN), Tehran, Iran
[f] Instituto Interuniversitario de Investigación de Reconocimiento Molecular y Desarrollo Tecnológico (IDM), Universitat Politècnica de València, Universitat de València, Valencia, Spain
[g] CIBER de Bioingeniería, Biomateriales y Nanomedicina, Instituto de Salud Carlos III, Spain
[h] Unidad Mixta UPV-CIPF de Investigación en Mecanismos de Enfermedades y Nanomedicina, Universitat Politècnica de València, Centro de Investigación Príncipe Felipe, Valencia, Spain
[i] School of Materials Science and Engineering, The University of New South Wales, Sydney, Australia
[j] Faculty of Mechanical Engineering, Tarbiat Modares University, Tehran, Iran
[k] Department of Chemical Engineering, Faculty of Engineering, Arak University, Arak, Iran
[l] Student Research Committee, Department of Pharmaceutics and Nanotechnology, School of Pharmacy, Shahid Beheshti University of Medical Sciences, Tehran, Iran
[m] Biionix Cluster, Department of Internal Medicine, College of Medicine, University of Central Florida, Orlando, FL, USA
[n] Department of Engineering, School of Science and Technology, Nottingham Trent University, Nottingham NG11 8NS, UK

ARTICLE INFO

Article history:
Received 10 June 2022
Received in revised form
2 August 2022
Accepted 12 August 2022
Available online xxx

Keywords:
Dendritic Mesoporous Silica Nanoparticles
Drug delivery
Biomolecules
Therapy
Diagnostic

ABSTRACT

Dendritic mesoporous silica nanoparticles (DMSNs) are a new generation of porous materials that have gained great attention compared to other mesoporous silicas due to attractive properties, including straightforward synthesis methods, modular surface chemistry, high surface area, tunable pore size, chemical inertness, particle size distribution, excellent biocompatibility, biodegradability, and high pore volume compared with conventional mesoporous materials. The last years have witnessed a blooming growth of the extensive utilization of DMSNs as an efficient platform in a broad spectrum of biomedical and industrial applications, such as catalysis, energy harvesting, biosensing, drug/gene delivery, imaging, theranostics, and tissue engineering. DMSNs are considered great candidates for nanomedicine applications due to their ease of surface functionalization for targeted and controlled therapeutic delivery, high therapeutic loading capacity, minimizing adverse effects, and enhancing biocompatibility. In this review, we will extensively detail state-of-the-art studies on recent advances in synthesis methods, structure, properties, and applications of DMSNs in the biomedical field with an emphasis on the different delivery routes, cargos, and targeting approaches and a wide range of therapeutic, diagnostic, tissue engineering, vaccination applications and challenges and future implications of DMSNs as cutting-edge technology in medicine.

1. Introduction

Nanotechnology utilizes nanostructures and nanophases to bridge the gap between biological and physical sciences. Nanoparticles (NPs) are synthesized for various applications such as theranostics, targeted therapy, drug delivery, tissue engineering, and regenerative medicine [1]. The most critical application for NPs in the biomedical field is drug delivery. NPs in the 10–400 nm

* Corresponding author.
** Corresponding author.
*** Corresponding author.
**** Corresponding author.
E-mail addresses: mehdi.razavi@ucf.edu (M. Razavi), mahdi.bodaghi@ntu.ac.uk (M. Bodaghi), t.kumeria@unsw.edu.au (T. Kumeria), rmaez@qim.upv.es (R. Martínez-Máñez).

https://doi.org/10.1016/j.mtchem.2022.101144

range have been widely used as advantageous drug carriers since they offer flexibility in carrying many different payloads, can provide enhanced blood circulation and active cell-targeting. In addition, NPs also avoid the low bioavailability of certain drugs and unfavorable pharmacokinetic parameters [2,3]. Several materials are utilized as nanocarriers for drug delivery applications, including chitosan, alginate, xanthan gum, cellulose, liposomes, polymeric micelles, dendrimers, nanocrystal inorganic nanoparticles, metallic nanoparticles, quantum dots, protein, and polysaccharide-based nanoparticles [4].

Drugs can be directly conjugated to the NP surface using surface chemistry or can be loaded within the NP's structure. A stimulus at the target site can also be utilized to trigger the release of the drug. In either of the above cases, it is essential to ensure that a therapeutic amount of drug is administered at the target site. To control the amount of drug released, NPs can be conjugated with targeting moieties that can take the advantage of ligand-receptor affinity to deliver the drug to the intended site [5]. The targeted receptor is often a protein overexpressed on the cell's surface in a specific disease condition. For instance, to deliver drugs to cancerous cells ligands such as folate, epidermal growth factor, transferrin, aptamers, antibodies, or antibody fragments were effectively utilized [4,6]. Several ligands have also been designed to deliver drugs in other diseases such as inflammatory mediators, neuropeptides, growth factors, and cytokines that can be used for atherosclerosis, Crohn's disease, arthritis, spondylitis, and other auto-immune disorders [7].

Among reported nanoparticles, dendritic mesoporous silica nanoparticles (DMSN) have been developed and used as drug carriers for different applications [8]. As the name suggests, DMSNs incorporate a mesoporous silica structure with radially symmetric, highly ordered branched structures [9]. DMSNs have superior biological properties and higher surface area than classical mesoporous silica nanoparticles. Moreover, DMSNs offer easy surface functionalization and have high specific pore volume that enables the encapsulation of large payloads. Pore sizes in DMSNs range from 2 to 50 nm and can be finely tuned for different applications [10]. Since pore sizes are key determinants, several researchers carried out systematic investigations to determine the pore sizes of dendritic NPs. In one such study, Haozheng et al. [11] used rigid NPs with tunable sizes as probes to detect the accessibility of the internal pore surface of dendritic porous NPs (DPSNs). Negatively charged NPs of different diameters were used as probes. They reported that DPSNs with central-radial pore channels have greater accessibility to the internal pore surface which affects the loading capacity significantly.

The Mobil Research and Development Corporation first reported the synthesis of mesoporous solids in 1992. These mesoporous structures were synthesized from silicate gels using the liquid crystal template mechanism [12]. A few years after, Cai and coworkers reported the synthesis of mesostructured silica with tunable particle morphologies. In their studies, the NPs so obtained were termed ‘radiolarian-like mesoporous silica nanoparticles. These were the first type of DMSNs reported [13,14]. In addition, the authors reported a bimodal pore size distribution attributed to micelles' dynamic self-assembly at the unstable oil-water interface during the synthesis. Moreover, DMSNs can be easily synthesized to have large internal pores with desired morphologies. Although in principle, the internal structure of DMSNs helps extensive biomolecular loading, large internal channels can also lead to drug leakage and thus reduce the amount of drug reaching the specific target site during *in vivo* delivery. Therefore, surface modification of the DMSNs is an important issue to block the pores to prevent the unwanted release of drugs. Recently, several surface modifications have been successfully incorporated to tackle the phenomenon mentioned above [15] for the final controlled delivery of metallic NPs, genes, vaccines, and catalysts [16–20]. The unique and flexible structure of DMSNs can therefore be leveraged to provide a reproducible, facile, and precisely controlled porous structure for diagnostics, therapeutics, and engineering applications [21–23].

The DMSNs may also be synthesized as organosilica NPs (DMSONs) that possess three-dimensional nanochannels that impart unique characteristics. Additionally, the incorporation of organosilica NPs improves biocompatibility, biodegradability, and hydrophobicity [24]. Similarly, Wang et al. synthesized dendritic fibrous nanoparticles (DFNPs) with central-radial nanochannels. Several studies found DFNPs to possess structural superiorities that enhance their candidature to serve as novel drug delivery platforms and nanocatalysts [25].

Hao et al. recently reported a review article on the synthesis procedures of DMSNs. The authors report elaborated methods of micro-emulsion templating, organosilane co-condensation, and spherical micelle self-aggregated assembly for synthesizing DMSNs [26]. Thananukul et al. summarized stimuli-responsive gatekeepers for porous nano-carrier drug delivery [27]. They briefly discussed the different templates and pore-forming agents like surfactants and amphiphilic block polymers. In another review, Du and colleagues recently discussed the catalytic and biomedical applications of micro-/nano-dendritic silica particles [28].

In the present review, we discuss the different routes of synthesizing DMSNs, the relevant properties, and different delivery routes that utilize complex targeting approaches to understand the underlying chemistry that makes them unique. Further, the article sheds light on the therapeutic applications of DMSNs using different payloads. Finally, we discuss their use as diagnostic tools, tissue engineering applications, safety considerations, and future perspectives to enable researchers to brainstorm ideas to utilize DMSNs for multimodal applications in an interdisciplinary approach. Although previous review articles have discussed the synthesis strategies of DMSNs and their potential chemical and biomedical applications, the present review dives in-depth into the synthesis strategies and lays a heavy emphasis on biomedical applications. This article spans various biomedical applications-gene delivery, multiple cancer and tumor mitigating strategies, use of DMSNs in vaccinations, tissue engineering, wound healing, and a comprehensive discussion of the safety and toxicity of DMSNs.

2. DSMNS as multifunctional nanocarriers

2.1. Synthesis methods, structural characteristics, and chemical properties

The development of ordered mesoporous materials MCM-41 [12] and SBA-15 [29], through a liquid crystal templating mechanism [30] pioneered the development of tunable porous silica materials and directed the development of diverse sol-gel methods to prepare ordered mesostructured with highly tunable porous silica frameworks with the help of cationic, anionic, or non-ionic surfactant as a template. The past three decades have shown rapid growth in the development of mesoporous silica with various topologies and architectures.

DMSNs present a unique structure that offers improved biological properties as a novel drug delivery platform able to encapsulate large payloads. The key advantages of DMSNs are mainly determined by their characteristic dendritic porous structure, with high surface area and tunable porosity [28]. Three main synthetic strategies have been described in the literature for DMSNs, *viz.* micro-emulsion templating (MET), organosilane assisted co-condensation (OAC), and spherical micelle self-aggregated assembly (SMSAA) (Fig. 1) [26]. In the MET approach, 3D-DMSNs are

prepared in a heterogeneous oil-water biphasic system with the silicate species in the oil phase and surfactant in the water phase using an organic base as a catalyst [31]. This biphasic system allows the reaction and facilitates assembly at the interface by altering or adding reactants in each phase without interrupting the interface (Fig. 1, a-d) [31]. Thus, this approach assisted in mesopore channel growth and swelling through silicate oligomer polymerization and condensation, forming new pore walls as a template (Fig. 1A, e-j) [31]. This procedure successfully achieved several generations of dendritic hierarchical mesostructures using a simple one-pot synthesis, in which pore size is tunable by changing hydrophobic solvents [31].

In the OAC approach, organotrialkoxysilane assisted by micelle/precursor co-templating assembly was utilized to design and synthesize dendritic mesoporous organosilica nanoparticles (DMONs) with uniform size, large nanopores, and small particle sizes [32]. This approach was exemplified by Wu et al., utilizing bis[3-(triethoxysilyl)propyl] tetrasulfide (BTES) as a bissilylated organosilica precursor to co-hydrolyze and co-condense organotrialkoxysilane for the preparation of DMONs [32]. The thioether-bridged organic group within BTES can be uniformly embedded with the framework (Fig. 1B a) as well as penetrate the hydrophobic domains of surfactant micelles (Fig. 1B b) resulting in enlarged micellar structure and pore size of DMONs [32].

In the SMSAA approach [33], a dual template synergistically controlled micelle self-aggregated model is utilized to form DMSNs (Fig. 1C). Here, cationic and anionic surfactants are premixed, resulting in mixed micelle aggregates (Fig. 1C i) [33]. Therefore, the anionic micelles are not used as a template but act against negatively charged silicate oligomer adsorption. Furthermore, under primary conditions, the hydrolysis and condensation of organotrialkoxysilane results in partially coated silica micelles (Fig. 2C ii) [33]. To minimize the interface energy, these micelles fused to form aggregates acting as a nucleus for the growth of the nanoparticles (Fig. 1C iii). This partially covered mono -, bi-, and aggregated micelles help form DMSNs (Fig. 1C iv) [33].

The large pore size associated with the DMSNPs is helpful for drug delivery applications, especially macromolecular payloads [34]. As an example, Dai et al. [35] (Fig. 2) fabricated DMSNs with a tunable pore size (~10 to ~35 nm) and high surface area prepared by the microemulsion approach using different amounts of the co-solvent mixture. Furthermore, the authors also demonstrated that guest nanoparticles such as copper sulfide (~10 nm), gold (~10 nm), and iron oxide (~25 nm) could be incorporated into DMSNs [35]. Pore size is an essential consideration for the loading of small molecules (drugs) or macromolecules (peptides, proteins, genes) on DMSNPs.

2.2. Biomacromolecules delivery

The biomacromolecules such as peptides, sugars, antibodies, proteins, and oligonucleotides [33,36,37], showed promising outcomes in treating common diseases. However, they introduce instability in systemic circulation and are susceptible to immune clearance and enzyme degradation [38,39], limiting their bioavailability in the target organs. Therefore, encapsulating these macromolecules in carries having a large pore size, such as DMSNs, is a promising strategy to protect them from such biological bottlenecks. The commonly used mesoporous silica nanoparticles of the MCM-41 type are not proper vehicles for encapsulating these large molecules because of their narrow pore size [40,41]. However, in mesoporous silica an increase in the diameter of pore channels usually causes an increase in the whole NP size, which is inappropriate for drug delivery applications [42].

DMSNs have shown effectiveness for the immobilization and encapsulation of enzymes, such as lipase [43,44], chloroperoxidase [45], laccase [46], cytochrome monooxygenases family [47], and glucosidases [48]. It is also applied in bio-catalysts with enhanced catalytic properties, enzyme stabilization, and functionality in the biomedical and industrial fields [49]. High protein loading capacity, highly accessible internal surface areas, and excellent biocompatibility are the most important features of DMSNs for the delivery of protein-based therapeutics [50]. DMSNs have also been used for protein delivery by oral administration despite their limited activity by degradation from gastrointestinal (GI) proteolytic enzymes and their permeation from barriers. An example is the delivery of insulin by dendritic mesopores of DMSNs functionalized with thiol-groups [51]. Results showed that pH-related degradation of this protein is significantly inhibited, and the transport of insulin successfully occurred. In the same way, D MSNs could be used for the delivery of prodrugs, and are able to tackle the physiological barriers against drug application, including lack of specificity, low oral drug absorption, chemical instability, toxicity, and poor patient acceptance (bad taste, odor, and pain at the injection site) [52].

In addition, human gene therapy (GT) is rapidly gaining popularity and due to this ample attention is received for the development of novel gene carriers. Currently, silica NPs-based GT suffers from low efficiency due to the passive-diffusion release of DNA and RNA. This can be attributed to the strong electrostatic interactions between negatively charged genes and positively charged NP surface. However, some of these problems can be avoided by utilizing large-pore DMSNs for loading genetic content.

A more recent antitumoral approach is based on immunotherapy, where the stimulation of the immune system was used for cancer cell elimination. Conventional adjuvants like MF59, aluminum salts, and ISA 206 are used for stimulating innate and secondary immunity. However, they can lead to toxicity-related safety concerns. For this reason, nanoparticles are being evaluated. Among them, dendritic hierarchical mesostructured silica nanoparticles have shown excellent properties for use as an adjuvant [19]. Uniform particle size accompanied by large pore size showed high protein loading capacity (376 μg mg^{-1}). Moreover, *in vivo* study on guinea pigs revealed no pathological abnormalities upon performing histology [19]. Besides, DMSNs have shown their superiority for loading cytokines, such as tumor necrosis factor-alpha (TNF-α), for stimulating the immune system, thus achieving effective anti-tumor efficacy while minimizing undesired side effects [53].

Cancer has several hallmarks including angiogenesis, mutations in controlling genes, uncontrolled cell growth, resistance to the natural cell death, cross-talks between cells, and activation of EMT pathways. Due to this complexity, a single strategy like chemotherapy may not be effective to induce the anti-tumor effect [54,55]. So, in the past decades, the results of numerous studies showed promising outcomes of combinatorial methods such as simultaneous delivery of two drugs, combination with genes or with novel therapeutic methods like photodynamic therapy (PDT) and photothermal therapy (PTT) [47]. These hybrid methods have produced an excellent platform for blocking more than one pathway in cancer development. DMSNs can play an important role in the combinatory delivery of a small drug such as doxorubicin with a big protein such as the interleukin-2 (IL-2) [56]. Additionally, DMSNs can be conjugated with photosensitizers with monoclonal antibodies (mAbs) for a dual chemo-PDT [57]. Finally, among the different payloads, NPs can be loaded into the DMSNs. For example, (Mn)-coupled dendritic mesoporous silicon nanoparticles also containing indocyanine green (ICG) and glucose oxidase (GOD) were successfully developed for tumor microenvironment (TME) remodeling and cancerous cells eradication [58].

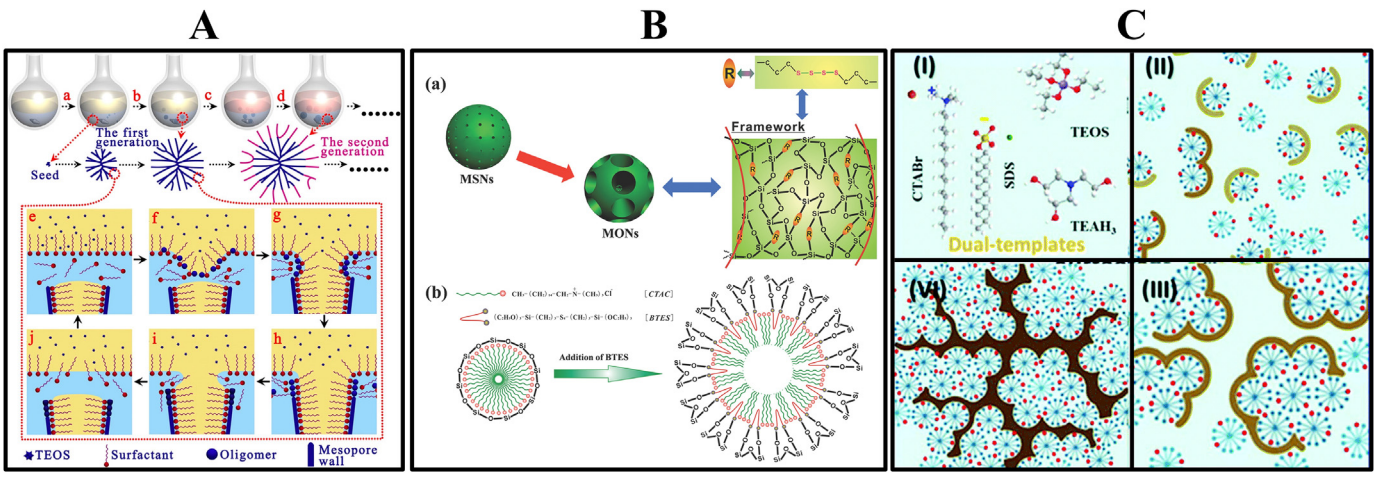

Fig. 1. Synthesis and proposed mechanisms of DMSNPs formation through A) micro-emulsion templating [31], B) organosilane assisted co-condensation [32], and C) spherical micelle self-aggregated assembly [33].

2.3. Stimuli-responsive delivery materials

As discussed above, the unique porous structure of DMSNs helps biomacromolecule delivery. However, large channels can also lead to important drug leakage and thus reduce the amount of cargo reaching the specific target site during *in vivo* delivery. Therefore, surface modification of the DMSNs is a critical issue to block the pores to prevent the unwanted release of drugs. Recently, several surface modifications have been successfully incorporated to tackle the phenomenon mentioned above [15] for the controlled delivery of metallic NPs, genes, vaccines, and, catalysts [16–18,20,47]. The unique and flexible structure of DMSNs can be leveraged to provide a reproducible, facile, and precisely controlled porous structure for diagnostics, therapeutics, and engineering applications [21–23].

Stimuli-responsive carriers offer a more accurate spatiotemporal targeting and dosage-controlled drug release. This concept is based on constructing a carrier that senses specific endogenous and exogenous stimuli and responds dynamically (E. Aznar 2016) (A. García Fernández, 2020). Depending on the stimulus, the smart carrier is guided and accumulated into a specific organ or undergoes a structural deformation and subsequently triggers the release of the loaded drug in a controlled manner [59–63]. The endogenous stimuli-responsive carriers are advantageous as changes in pH, redox potential, and specific enzyme concentration can usually be found between the targeted and off-target tissue/cells. On the other hand, exogenous stimuli-responsive carriers have also been described using temperature, light, electric field, alternating magnetic field (AMF), and ultrasound (Fig. 3) [64,65]. Table 1 lists a summary of various external and internal drug release stimuli and their mechanism of action, pros, and cons.

Endogenous stimuli-responsive carriers have been widely evaluated for triggered drug release applications. pH-responsive carriers have been applied as drug delivery systems to specific organs (e.g., the vagina or the gastrointestinal tract) or intracellular compartments (e.g., lysosomes or endosomes), or pathological situations, such as inflammation or cancer. Constructing pH-responsive drug delivery systems is usually based on two approaches: the utilization of molecules with ionizable groups and the utilization of pH-labile bonds in the structure of the pH-responsive carrier. For instance, amino DMSNs were synthesized

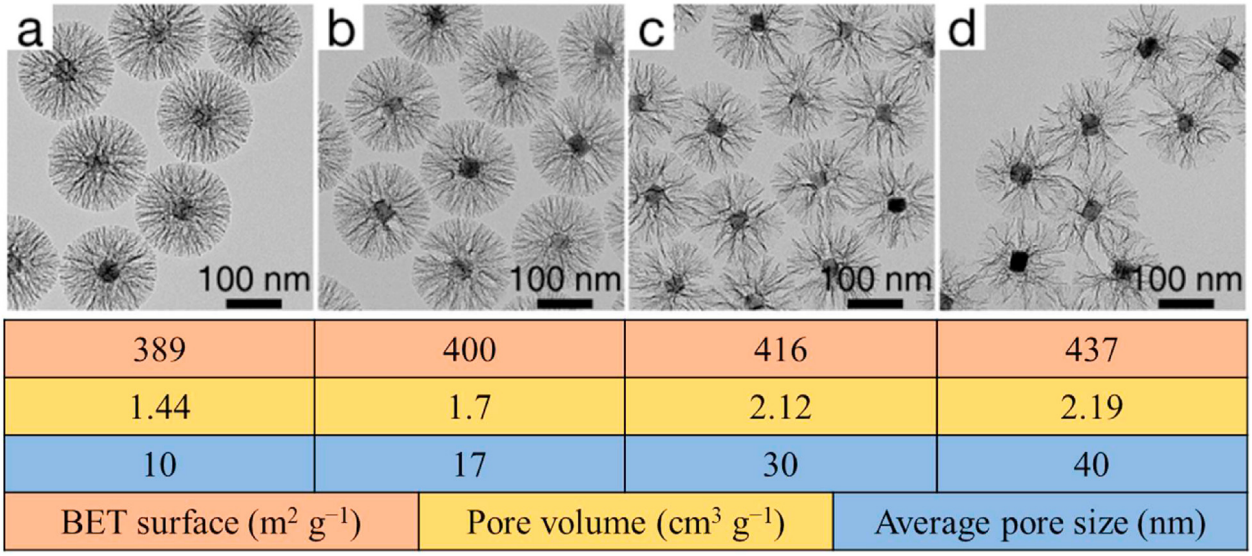

Fig. 2. DMSNs are fabricated with different pore sizes, pore volumes, and BET surface using different amounts of the co-solvent mixture [35].

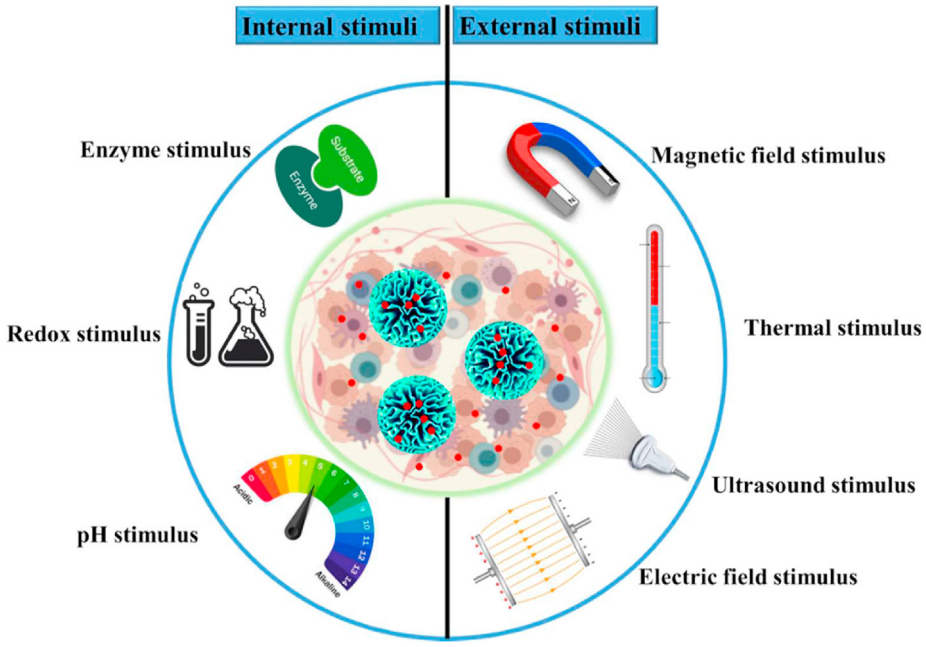

Fig. 3. Internal and external stimuli are applicable in active drug delivery systems.

as pH-responsive carriers for cyclometallated gold(III) delivery. The amino groups formed weak hydrogen bond interactions with cyclometallated gold(III). At acidic pH, the functional groups protonated and promoted the release of the loaded drug [66]. Curcumin (Cur) was also loaded into the pores of DMSN-decorated reduced graphene oxide (rGO) and observed a significant drug release at acidic pH due to weakening the electrostatic interaction between the drug and DMSNs. Cur is a herbal supplement, cosmetics ingredient, food flavoring, and food coloring (bright yellow) chemical agent produced by plants of the Curcuma longa species. There are numerous reports, which have shown its anticancer, antioxidant, anti-bacterial, and many different other functions of this potent herbal extract in formulation with different nanocomplexes. The most important reason for using nanoformulation of this magic extract is its low bioavailability, due to its negligible hydrophilicity [67]. Fan et al. synthesized magnetic core-shell NPs composed of cobalt ferrite@dendritic mesoporous silica shell and doxorubicin (DOX) was loaded into the pores through hydrogen bonds interactions between silanol groups (Si—OH) of DMSNs and carboxylic groups of DOX. The authors observed drug release under acidic conditions caused by weakening hydrogen bonds and electrostatic interaction between the drug and the carrier, and enhanced DOX's hydrophilicity due to its ammonium groups' protonation [68].

Huang et al. [69] synthesized pH-responsive DMSNs using vinyltriethoxysilane as a precursor to synthesize vinyl modified DMSNs. Subsequently, DOX was conjugated to the vinyl-modified DMSNs through acid-liable hydrazone bonds (Scheme 1). Delivery studies demonstrated that the cumulative release of DOX in acidic conditions (pH 5.3) was higher than in neutral conditions (pH 7.4) due to the cleavage of the hydrazone moieties. Wang et al. [70] synthesized pH-responsive DMSNs loaded with Cur for breast cancer treatment. In this case, the authors modified DMSNs with calcium hydroxide which was conjugated with curcumin through chelating interactions with divalent calcium. The results showed that Cur release reached up to 80% in 0.5 h under acidic conditions, which was significantly higher than that found in neutral conditions (35% release) after 12 h. Li et al. [69] used a Schiff-base linkage to synthesize DMSNs for co-delivery of DOX and shRNA-expressing plasmid (pDNA). The authors observed an acidic pH-dependent drug and pDNA release. Besides, imidazole modification of DMSN provided endosomal escape via a proton sponge effect.

Most of the redox-responsive drug delivery systems are based on the potential of glutathione (GSH) to cleave disulfide bonds, taking advantage of the different GSH concentrations found in intracellular (~2–10 mM) and extracellular (~2–10 μM) compartments, and in healthy tissues compared with tumor ones. Yang et al. [70] used 1,4-bis (triethoxysilyl)-propane tetrasulfide (BTES) as the precursor to homogeneously distribute disulfide groups into a hybrid framework of DMSNs to synthesize GSH-dependent degradable NPs. They observed that the NPs degradation in cancer cells was faster than in normal cells due to the higher GSH concentration in the former. The authors also found a pore size-dependent degradation with a higher degradation in nanoparticles with larger pore sizes. Lu et al. [71] followed a similar approach to synthesize a self-adjuvant and co-delivery system for cancer immunotherapy. As above, BTES was used to provide a GSH-dependent degradable behavior to the NPs and the system was loaded with a toll-like receptor 9 (TLR9) and an antigen (ovalbumin). The authors also included PEI in the NPs to induce endosomal escape through the proton sponge effect. The synthesized NPs could effectively escape from the endosome and deliver the loaded cargos to antigen-presenting cells (APCs). *In vivo* studies indicated that the administrated NPs reduced the intracellular GSH level by disturbing ROS-GSH balance and subsequently enhanced the proliferation of cytotoxic T lymphocytes (CTL) to suppress tumor growth. Despite the usability of DMSNs and similar NPs in drug delivery systems, their long *in vivo* retention, difficult degradability, and toxicity causes severe shortcomings. One way to circumvent this issue is by introducing disulfide bridges (as mentioned in the previous study). Once the tumor cells take up the NPs with disulfide bridges, the bridges are cleaved by a high concentration of glutathione and cause a release of cargo. Du et al. have comprehensively summarized disulfide-bridged frameworks and their applications in a recent review article [72].

Table 1
A summary of various external and internal drug release stimuli and their mechanism of action, pros, and cons [64,87–89].

		Mechanism	Pros	Cons
External stimuli	Thermo-Responsive Systems	High mobility of matrix phase transition in polymers above or below defined temperatures	Facile implementation of active moieties Facile formulation and manufacturing	Instability of thermolabile drugs Sensitive to environmental changes Possible harmful effects on healthy cells
	Ultrasound	The thermal and mechanical effects generated by cavitation phenomena or radiation forces	Significant penetration deep Easily adjusted Low cost Local and focused heat induction Insensitive to surrounding medium	Difficulty to target moving organs Difficulty in exposing large zones High reflection at the bone (60%) and air (99%) interface High absorption in bone Expensive equipment for controlled release
	Light-responsive Systems	Photothermal mechanism, upconversion mechanism, and two-photon activation mechanism	Very precise Easily tuned Low cost Spatiotemporal targeting	Low tissue penetration (can be improved by using NIR light) For deep tissues: invasive UV: harmful Inconsistent responses to light
	Electro-Responsive Systems	Electrochemical reduction−oxidation and electric-field-driven movement of charged molecules Electrostatic interactions variability	Pulsative release with changes in electric current Spatiotemporal targeting	Invasive implantation required Required additional equipment for external administration of stimulus Hard to optimize the magnitude of electric current Poor penetration deep Sensitive to the surrounding environment
	AMF-Responsive Systems	Magnetic-guided localization Magnetic hyperthermia Structural instability through MNPs fluctuation	Magnetic field-induced particles accumulation Energy conversion with an alternating magnetic field Noninvasiveness High tissue penetration Spatiotemporal targeting Insensitive to the surrounding environment	Embolism or toxicity through the particles accumulation Expensive and complex facilities Large facilities
Internal stimuli	pH-Responsive Systems	Ionization of basic or acidic groups Cleavage of acid-sensitive bonds	Ease of implementation pH difference in the human body Controlled drug release Subcellular drug delivery	Not suitable in biosystems when adding acid and base Polymer-dependent toxicity Poor conjugate bioactivity Poor mechanical strength
	Enzyme-responsive Systems	site-specific enzymatic cleavage	Enzyme specificity Protection of drugs in blood circulation Tumor-selective accumulation Controlled drug release Improved pharmacokinetic	Enzyme dysregulations in diseases Heterogeneous spatial and temporal patterns of enzyme activity Substrates overlap for closely related enzyme families Complexity in the large-scale production
	Redox-responsive Systems	Disulfide bonds cleavage by glutathione (GSH)	Normal tissues Stability Prompted response to a high concentration of GSH (usually a few minutes to hours) Cytoplasmic drug delivery	Tumor cells heterogeneities Complex biological environment

In another approach, Fei et al. [73] synthesized a smart redox-responsive co-delivery system for a therapeutic model gene (Bcl-2 siRNA) and small-molecule anticancer drug (SN-38). The cyclodextrin-conjugated PAMAM dendrimers were applied to enhance the loading capacity of B-cell lymphoma-2 (Bcl-2) siRNA and SN-38 through the electrostatic attraction and host-guest interaction, respectively. First, the authors conjugated nitrophenyl-benzyl-carbonate, a ROS-responsive substance, on the pore rims of DMSNs. Next, the dendrimers were attached to DMSNs via a redox-sensitive ligand (azido ligand). The data indicated that the synthesized nanoplatform was successfully internalized into 4T1 cancer cells, escaped from the endo/lysosome compartments, and released the loaded drug into the cytosol. Redox-responsive DMSNs have also been used for molecular imaging of the cellular trafficking of NPs into cells. In this frame, Du et al. [74] used an acetaldehyde-modified-cystine (AC) linker, a GSH-responsive autofluorescent reporter agent containing disulfide bonds to graft PEI on amino-functionalized DMSNs. In this case, the reduction in fluorescent signal intensity of AC under interaction with cytosolic GSH revealed the internalization of the vehicle. Increasing GSH concentration reduced the fluorescent intensity.

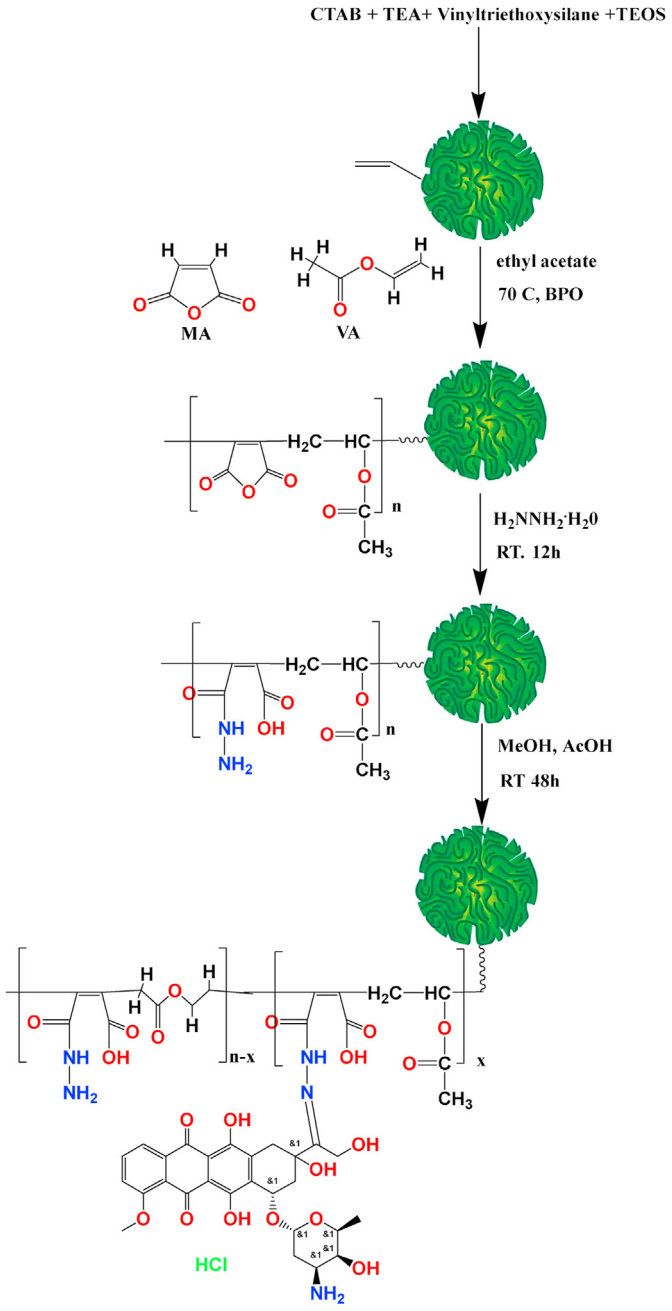

Scheme 1. Reaction scheme for the synthesis of pH-responsive DMSNs for the delivery of DOX using acid-responsive hydrazone bonds. CTAB: Cetrimonium bromide, TEA: Triethanolamine, TEOS: Tetraethoxysilane, MA: Maleic anhydride, VA: Vinyl acetate, BPO: Benzoyl peroxide, RT: Room temperature.

Temperature-responsive carriers are usually based on the use of thermal-responsive polymers used as gatekeepers. At a temperature higher than the critical temperature, the expansion or collapse of polymer chains occurs due to disruption of the intramolecular and intermolecular hydrophobic and electrostatic interactions of the polymer chains.

Regarding external stimuli, light-responsive carriers have shown promising results in on-demand drug delivery approaches. In this case, light-responsive structures undergo structural changes under interaction with light having specific wavelengths, such as ultraviolet (UV), near-infra-red (NIR), or visible. Basically, three different mechanisms have been proposed for light-induced structural changes, including the photothermal effect, upconversion effect, and two-photon activation. The photothermal effect is based on the conversion of light energy to heat that finally affects temperature-responsive structures. The up-conversion effect is based on the absorption of NIR light via specific materials and the emission of UV light that then affect UV-sensitive systems. A similar approach can be flowed using two-photon activation [70,75,76]. In the case of using ultrasound, the waves can not only trigger drug release from specific carriers but also transient increase in vessel permeability, providing both on-demand drug release and carrier accumulation in the tumor [77,78].

Electric field as a stimulus is usually applied as an external drug release trigger. Different mechanisms are involved in the electrical drug release stimulation, such as electrochemical oxidation-reduction, changes in electrostatic interactions, and electric-field-driven displacement of charged moieties [78,79]. Magnetically-responsive systems have shown promising results in both magnetically guided carrier localization and magnetically triggered drug release. Typically magnetic responsive systems incorporate a magnetic agent, such as magnetite (Fe_3O_4) or maghemite (Fe_2O_3) NPs [80,81]. Furthermore, thermal generation by MNPs through the Néel and Brownian relaxation is another possible mechanism to trigger drug release from thermo-responsive structures [82].

In these DMSNs, the stimuli-responsive ensembles are usually attached to the surface serving as pore gatekeepers. Substances such as Poly(N-isopropyl acrylamide) (PNIPAM), poly(*N, N*-diethyl acrylamide) (PDEAAm), poly(N-vinyl caprolactam) (PVCL), and poly [2-(dimethylamino)ethyl methacrylate] (PDMAEMA) for thermal-responsive material [83], azobenzene group, spiropyran–merocyanine, thymine, and o-nitro benzyl for light-responsive systems, polypyrrole, ethylene vinyl acetate, polyaniline, polythiophene, and polyethylene for electro-responsive materials [79,84,85] and magnetic nanoparticles (MNPs) for magnetic-responsive systems can be used. In an example [86], dendritic Silica/Titania mesoporous NPs loaded with curcumin were used for a targeted synergetic chemo-sonodynamic therapy. PEI-FA was attached to NPs through electrostatic interaction as a gatekeeper and active targeting agent. In the synthesized system, the TiO_2 layer serves as the sonosensitizer agent generating free radicals, $OH^{\cdot}$ and O_2^{-}, under exposure to ultrasound. The generated free radicals cut off the PEI gatekeeper and release the loaded Cur.

3. Administration and long-term circulation of DMSNs

Tailored nanostructures can be used as carriers and loaded/conjugated/adsorbed with various small molecules, natural substances, and diagnosis agents for therapeutic and diagnostic applications [90,91]. Additionally, these nanocarriers can be employed to deliver cargos through different routes, such as oral, intravenous, intraperitoneal, intratumor, and transdermal routes [92–98]. In this scenario, nanostructures should be appropriately designed, fabricated, and modified concerning the intended application and target cell/tissue/organ to be reached. Accordingly, DMSNs offer tunable physicochemical properties with unique characteristics [26,99]. After intravenous or intraperitoneal injection, a systemic distribution is observed in the bloodstream with preferential accumulation on major target organs (liver, lung, kidneys, spleen), attributed to their high capacity to retain foreign substances. Besides, DMSNs have also been applied locally in cancer therapy through intratumoral injection, in skin treatments as topical formulation [100], and for gastrointestinal delivery (GI) (see Table 2) [101] (see Table 3).

Regarding systemic administration, the ability of nanoparticles to accumulate in tumors has been reported. This phenomenon is called passive targeting and it is related to the so-named enhanced

Table 2
Examples of DMSNs in drug delivery applications and different delivery routes.

Chemical compound	Nanoparticle	Delivery routes	Effects
Omeprazole	DMSNs	Oral	Increased solubility and bioavailability, passing through the small intestine [101]
Insulin	DMSNs	Oral	Enhanced insulin transport in the intestine [51]
Exenatide	DMSNs	Oral	Improved loading and decreased burst release [102]
Gold (Au) and tantalum oxide (TaOx)	DMSNs	Injection- peritoneal cavity	The enhanced contrast agent improved image quality and radiotherapy treatment [103]
Curcumin	DMSNs	Injection- peritoneal cavity	Increased functionality and bioavailability [70]
Paclitaxel	DMSNs	Injection- peritoneal cavity	Improved drug loading and stability, decreased cytotoxicity [104]
Demethylcantharidin	DMSNs	Injection-intratumor	Improved cancerous cell growth control without side effects on healthy tissues [105]
Indocyanine Green (ICG) and natural glucose oxidase (GOD)	manganese etched DMSNs (DMMnSiO3 NPs)	Injection-intratumor	Controlled cell proliferation, and enhanced effect of photothermal therapy [106]
Iron oxychloride (FeOCl)	(H-DMOS)	Injection- Intravenous	Inhibitory effect on the growth of cancerous cells [107]
copper peroxide nanodots, chlorin e6 (Ce6), and polyethylene glycol	UMNOCC	Injection- Intravenous	Notable tumor cell apoptosis due to simultaneous NO generation and Fenton-like reaction [108]
Doxorubicin (dox), all-trans retinoic acid (ATRA), and interleukin-2 (IL-2)	DMSNs	Injection- Intravenous	Low systematic toxicity, increased tumor inhibitory effect due to the synergetic co-delivery [56]
5-HM, (5-hydroxymethylfurfural)	DMSNs	Direct	Increased bioavailability [100]

permeation and retention (EPR) effect. It is well known that the blood vessels and junctions in tumor tissue are distinct from normal tissue due to prevailing inflammation/hypoxia conditions [109,110]. During the fast growth and hypoxia, cancer cells secret some angiogenesis factors such as vascular endothelial growth factor (VEGF) and basic fibroblast growth factor (bFGF) to mediate a high level of angiogenesis. Accordingly, the newly formed vessels are fenestrated and leaky. The endothelial cell junctions are loose, enhancing permeability and extravasation of NPs with specific sizes from the tumor vasculature into the tumor interstitium [111,112]. In the same direction, impaired lymphatic drainage in tumor tissue contributes to NPs retention. Although the exact size for the passive targeting approach is not known, it is reported that the EPR effect is beneficial for the accumulation of macromolecules larger than 40 kDa or particles of diameter ~20–500 nm [109,110].

DMSNs with tunable size and surface characteristics can be extravasated into tumor tissues through the EPR effect. The EPR effect and its efficacy for targeting applications can vary between tumors and are highly dependent on intrinsic tumor biology factors such as intratumor pressure, degree of lymphangiogenesis and angiogenesis, the density of the stromal response, tumor cell growth gradient, and the degree of perivascular tumor growth (Fig. 4) [110,113]. Moreover, in a recent study by Sindhwani et al. [114] the authors confirmed the entry of the nanoparticles into the tumors by an active process across endothelial cells rather than through inter-endothelial gaps. The authors evaluated and confirmed their observation using different mouse models of human tumors, various imaging modalities, modeling, and simulation approaches. These observations comprehensively explain the exact mechanisms underlying the “passive” uptake of NPs.

Table 3
The common tumor marker, the overexpressing organs, and corresponding targeting agents.

Tumor marker	Overexpression in various tumors	Targeting agent	Ref
EGFR	Glioma (40–60%) Colon (50%) Head and neck (90–100%) Lunge (45–80%) Pancreas (22–60%) Prostate (60–89%)	Cetuximab scFv 425 Nanobody 8B6 Nanobody D10 EGF	[139]
HER2	Breast Cancer (15–30% in invasive form) Gastric Cancer (10–30%) Esophageal Cancer (0–83%) Ovarian Cancer (20–30%) Endometrial Cancer (14–80%) Lunge Cancers (20%) Urothelial Bladder Carcinomas (23–80%)	Nanobody 2Rs15d scFv 4D5 Affibody ABY-025 Pertuzumab Trastuzumab (Herceptin) Fam-trastuzumab-Deruxtecan	[140]
HER3	Breast cancer	Epidermal growth factor receptor EGFR	[141]
Cellular adhesion molecules, such as αvβ3-integrin	Vasculature endothelial cells in solid tumors	RGD	[142]
PDGFR β	1. Endothelial cells 2. Tumor-associated stromal cells 3. Melanomas(50–60%)	1. Vascular Endothelial Growth Factor(VEGF) 2. Epidermal growth factor receptor (EGFR), vascular endothelial growth factor receptor 2 (VEGFR2) 3. Multiple G-quadruplexes	[143–145]
IGF-1R	breast cancer prostate	Insulin and insulin-like growth factor (IGF)	[146]
TfR (Transferrin receptor	Leukemia Lung Prostate Ovarian Liver Colon Breast Brain	HAIYPR (T_7)peptide, PAMAM-PEG-T7/DOX nanoparticles	[147]
PSMA	Prostate epithelium(94.1%)	In-DTPA-D2B-IRDye700DX	[148]
Carbohydrate moieties	Lung	monoclonal antibodies	[149]
Mesothelin	Ovarian Pancreatic cholangiocarcinoma	chimeric monoclonal antibody	[150]
IL-13Rα2	pulmonary fibrosis	Glioblastoma multiforme (GBM)	[151,152]
FRα	Ovarian 93% Endometrial 90% Renal 50% Lunge 33% Colorectal 22% Breast 21%	folate	[153]
FSHR	vessel endothelial cells prostate	follicle	[154]
CD3	Head Neck Colorectal	HER2	[155]
CD19	B cells in the bone marrow	Chimeric antigen receptors T cell	[156]

The synthesized nanocarriers must have longer blood circulation times to accumulate at the intended site of action. The non-specific uptake and fast clearance of intravenously injected nanocarriers by the opsonization/phagocytosis process and reticuloendothelial system (RES) cells are the most critical issues shortening the blood circulation time/half-life [115,116]. The opsonization of nanocarriers by the blood plasma proteins, mainly albumins, complement proteins, immunoglobulins, fibronectins, fibrinogens, and apolipoproteins, also limits their ability to accumulate at the target site. In addition, nanocarriers can be visible to phagocytic cells (e.g., neutrophils, monocytes, macrophages, and dendritic cells) [117,118]. Nanostructure's surface properties, such as hydrophobicity, functional groups, and charge, have determinant roles in the opsonization process. Hydrophilic and neutral surface charges are more prone to escape opsonization compared to hydrophobic and charged surfaces. Alternatively, the surface of nanostructures can be modified with proper polymers, such as polyethylene glycols (PEGs), dextran, and poly(N-(2-hydroxypropyl)methacrylamide) (poly(HPMA)) [119,120].

Pegylation is one of the most efficient and well-established approaches to modifying nanostructures' surfaces to mask them from opsonization and extend their blood circulation time/half-life. In this scenario, conjugated/adsorbed PEG polymer provides a steric barrier on the nanostructure's surface. It repels blood plasma proteins, cells, and other biomolecules [121,122]. Pegylation of silica nanoparticles (NPs) has been extensively evaluated and conducted using various methods. The electrostatic self-assembly (of PEG on NPs is a straightforward and efficient Pegylation process [123]. Thierry et al. [124] synthesized porous silica NPs physically decorated with polyethyleneimine (PEI)-PEG copolymer and reported that the surface modification increased colloidal stability in the biological condition and reduced the nonspecific fouling via blood serum proteins. Despite its simplicity and low cost, the physisorption methods suffer from low stability and vulnerability to thermal, ionic strength, and pH of suspending media [125,126]. Apart from the physisorption, some chemical conjugation methods are applicable for the Pegylation of DMSNs (Fig. 5), including PEG-silane, amine-NHS coupling, and thiol-carboxylate coupling, thiol-

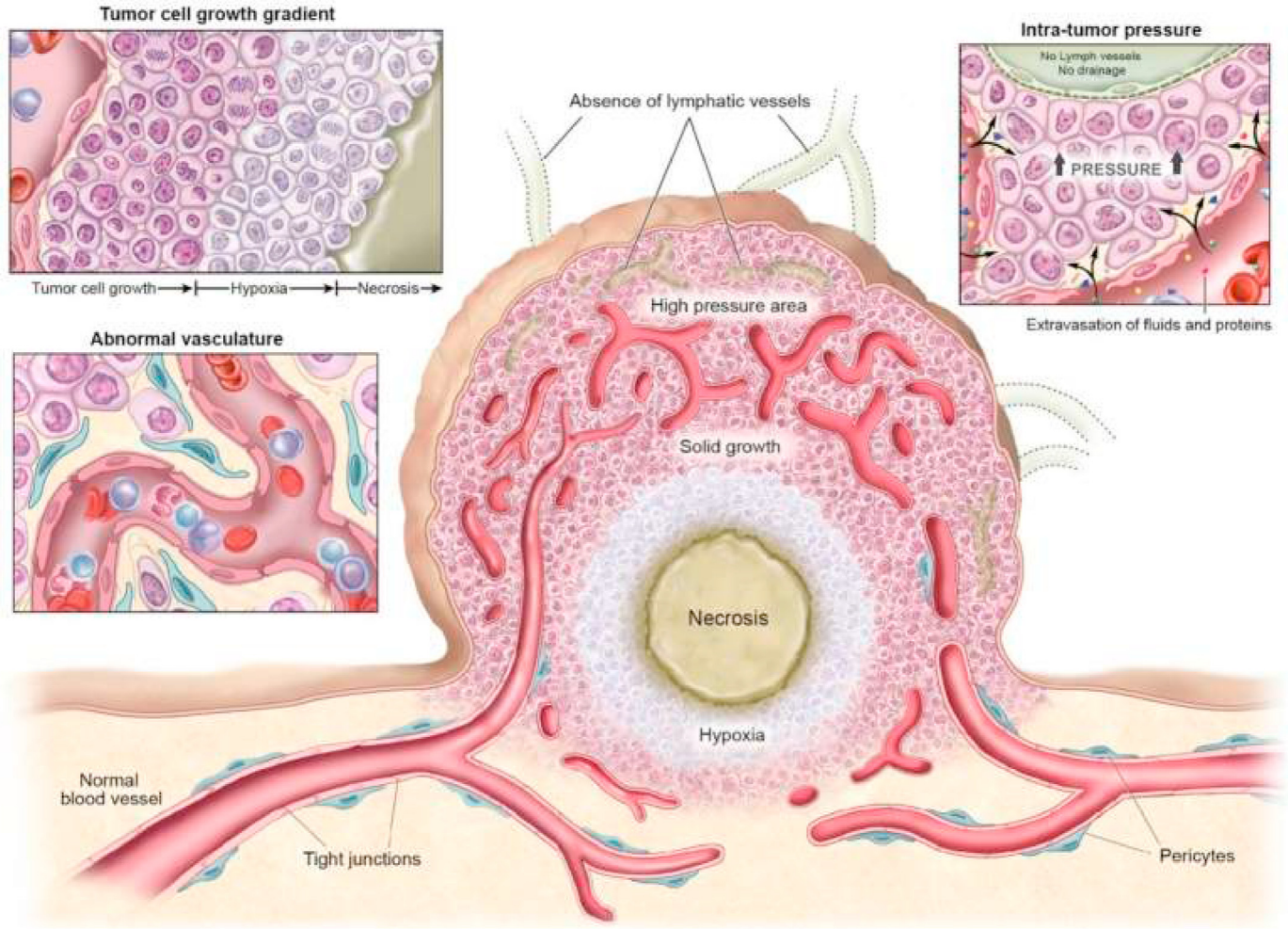

Fig. 4. Physiological properties of tumor tissue and vasculatures that can facilitate or prevent cancer drug delivery. Reproduced with permission from [114].

maleimide coupling, epoxy-amine coupling, and isocyanate-amine coupling methods. With the advent of multifunctional PEG, it is possible to decorate DMSNs and conjugate targeting agents onto the incorporated PEG polymer chain [127,128].

Furthermore, with the proper implementation of spatiotemporal targeting approaches, nanostructures can enhance the accumulation of the loaded drugs at the desired place, preserve drug leakage, eliminate off-target effects and provide controlled drug release [129,130]. Specific targeting of the nanoformulations towards the desired site of action and controlled cargo delivery is conducted through active targeting, and by implementing stimuli-responsive approaches. Although the passive and active targeting concepts are designed to accumulate the loaded therapeutic/diagnosis agents at the site of action and provide spatial targeting, the stimuli-responsive systems provide temporal targeting in addition to spatial targeting [109,131]. Notably, it is possible to apply different spatiotemporal targeting strategies to DMSNs due to tunable size and well-established conjugation chemistry.

Different surface functionalization strategies with specific ligand/targeting agents for active targeting have been described showing a significant increase in the accumulation, retention, and internalization of NPs into the targeted cells [132,133]. The active targeting approach is complementary to the passive delivery concept. The conjugated/attached ligand/targeting agents are associated with specific receptors or molecules overexpressed in diseased tissues, cells, or subcellular domains. Accordingly, the implementation of active targeting reduces the required injection dose and it protects non-targeted normal tissues from the side toxicity of nanoformulations [134,135]. Choosing a proper targeting agent and the conjugation process are the most critical factors determining the efficacy of targeting. The candidate tumor marker should be overexpressed explicitly in the target tumor, possess a relatively high and specific affinity to the conjugated/attached ligand/targeting agent, and be accessible. Various targeting agents made from carbohydrates (e.g., glucose, galactose, mannose, and dextran), antibodies, nanobodies, cell surface receptors, vitamins (e.g., vitamin D and folate), and aptamers have been evaluated for active targeting applications [110,136–138].

In terms of the conjugation process, the conjugation must be stable. In addition, the conjugation/attachment process should be straightforward, facile, effective, and compatible with the targeting agent. Broadly, the conjugation/attachment procedures targeting agents on DMSNs are divided into physisorption and chemisorption methods [157,158]. Physisorption methods are based on the physical interactions between the targeting agent and DMSNs surfaces, such as electrostatic interactions and hydrophobic interactions [126,159,160]. Although they are partially straightforward and conducted in the mild experimental conditions, they suffer from poor reproducibility, random orientation, low stability, and susceptibility to environmental conditions, such as temperature, pH, and ionic strength of the medium. In a study [86], positively charged PEI-FA was conjugated, via electrostatic interaction, on negatively

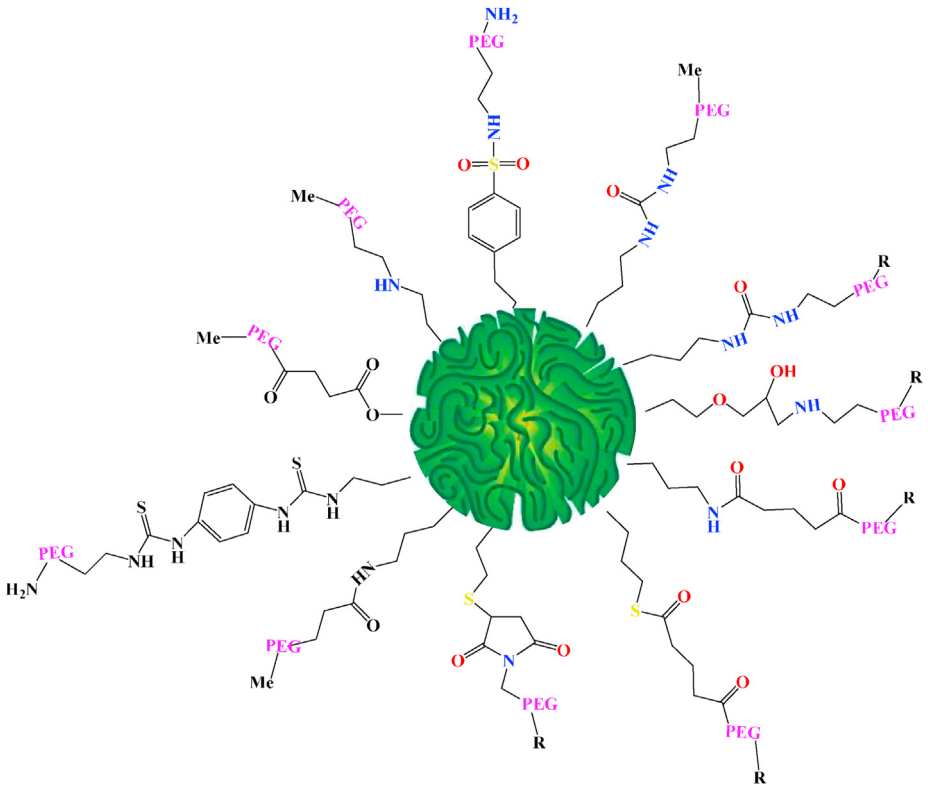

Fig. 5. Illustration of the different grafting methods used for PEGylation.

charged TiO_2-coated, Cur-loaded DMSNs. The PEI-FA served not only as the surface modifier but also as the gatekeeper agent preventing curcumin release from the TiO_2-coated DMSNs pores. The results showed that the cytotoxic effects of FA conjugated NPs on HeLa cells, folate receptor overexpressing cell, was significantly higher than that of A549 cells, folate receptor-negative cells.

On the other hand, the chemisorption beneficiates from the chemical reactions between the DMSNs surface and the targeting agents. In this scenario, the surface of DMSNs should possess functional groups for the intended chemical reaction. DMSNs are relatively easy to functionalize due to multiple silanol groups (Si—OH) on the surface. These silanol groups can be modified for different conjugation methods. The induction of functional silanes on the DMSNs through either co-condensation or afetr-synthetic grafting is a practical approach for targeting agent conjugation [161]. The co-condensation method generates the functional silanes on the DMSN's surface and inside the pores of the DMSNs. At the same time, after-synthetic grafting generates the functional groups mainly on the surface. The conjugation of targeting agents on DMSNs can be conducted utilizing some commercially available crosslinking agents, such as maleimide-PEG-N-hydroxysuccinimide (Mal-PEG-NHS) ester, m-maleimidobenzoyl-N-hydroxysuccinimide ester (MBS), and N-(a-maleimidoacetoxy)succinimide ester (AMAS) (Fig. 6) [127,162].

The induced functional groups can be utilized for further conjugation of different targeting agents. For example, Cai et al. [163] conjugated triphenylphosphine (TPP), a mitochondria-targeting ligand, to Pt-decorated DMSNs for photodynamic therapy (PDT) applications. They used 1-ethyl-3-(3-dimethyl amino-propyl) carbodiimide (EDC)/N-hydroxysuccinimide (NHS) coupling chemistry to attach TPP on DMSNs. The authors reported that the synthesized nanoplatform showed an enhanced PDT effect. Folic acid receptors (FRs) are highly overexpressed in different cancers and have a high affinity to its ligand, making folic acid (FA) a promising targeting agent. Accordingly, a lot of attention has been given to developing folate conjugated NPs as active targeting agents. In a study, Wang et al. [70] used APTES to include NH_2 functional groups on curcumin-loaded DMSNs and applied the EDC/NHS coupling chemistry to conjugate FA. They reported that DMSNs increased Cur-induced intracellular ROS generation and MCF-7 apoptosis rate. In another study, Dai et al. [164] applied the same approach, APTES surface modification, and EDC/NHS coupling chemistry, to conjugate FA on doxorubicin-loaded DMSNs (DOX@DMSNs). The authors also used *N, N*-phenylene bis-(salicylideneimine)dicarboxylic acid (Salphdc) as both, a gatekeeper and as a fluorescence imaging probe. They reported that the synthesized DOX@DMSNs were internalized by HepG2 cells through the FA receptor-mediated endocytosis process. Studies on a liver tumor-bearing nude mouse model showed that DOX@HPSN−Salphdc−FA administration induced better curative results than the control (PBS and free DMSNs) and free DOX (Fig. 7 A, B, and C). Moreover, biodistribution studies (Fig. 7 D, E, and F) revealed that the DOX@HPSN−Salphdc−FA effectively accumulated into tumor tissue and the efficacy of DOX@HPSN−Salphdc−FA for tumor targeting was significantly higher ($p<0.01$) than that of non-targeted NPs (DOX@HPSN−Salphdc).

4. Diagnostic applications

4.1. Imaging

The application of magnetic NPs and mesoporous silica nanoparticles has attained much attention since these NPs can provide tunable innovative imaging properties that can be utilized in

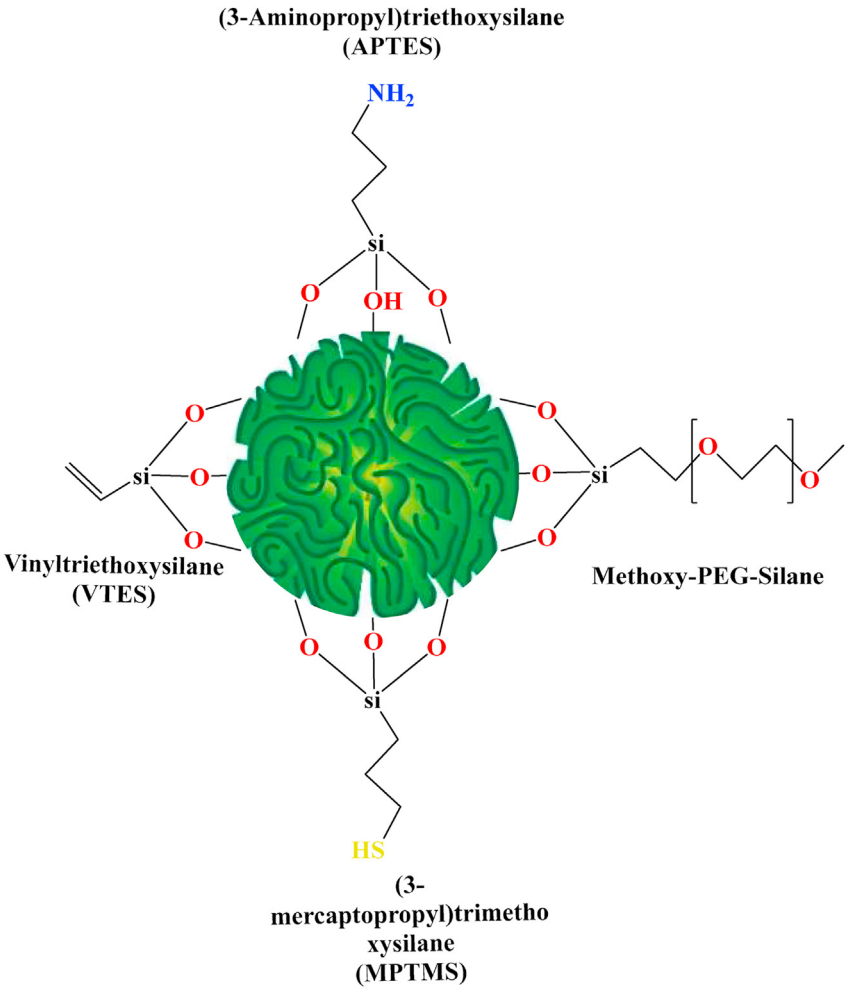

Fig. 6. Chemical structure of commonly used organosilanes.

different diagnostic and therapeutic applications [106,165]. Flood-Garibay and Méndez-Rojas [165] synthesized magnetic wrinkled mesoporous silica nanoparticles (MWMSNs) with two separate methods. In the first approach, the magnetic NPs were included during the preparation of the WMSNs, and in the second procedure, magnetic NPs and WMSNs were mixed using ultrasound waves. The first method resulted in core-shell magnetic nanoparticles, while the second resulted in WMSNs containing magnetic NPs on the surface. Both particles had excellent magnetic properties and could effortlessly be separated by an external magnetic field from aqueous suspension, and showed great potential in applications like imaging contrast agents and targeted drug delivery [165]. Li et al. [107] reported the combination of FeOCl as a contrast agent for T2-weighted MR imaging with dendritic mesoporous organo-silicon. The nanoparticles were used to improve the restriction of the Fenton reaction in chemodynamic cancer therapy for imaging [166]. Up-conversion dendritic mesoporous silica NPs encapsulating copper peroxide have also been prepared and used in cancer treatment and imaging applications [108].

4.2. Diagnostic assays and adsorption applications

The tunable characteristics of DMSNs make them great candidates for various biological applications. DMSNs have a large surface area with adjustable pore diameter and a large volume of radial porous channels that provide many sites for the functionalization of miscellaneous molecules like proteins, peptides, and enzymes [22,167,168]. The specific surface modification of the DMSNs can be applied in the fields of diagnosis or sensing of particular molecules. DMSNs have been used in immobilizing enzymes to improve the signal in detection tests (Fig. 8A and B). The large surface area and large porosity of the DMSNs enable them to encapsulate high levels of biomolecules. Moreover, the large porosity of the DMSNs provides a large contact area between the substrate and the encapsulated biomolecule. Based on this, Lei et al. [22] loaded horseradish peroxidase (HRP) inside the DMSNs to increase insulin detection. The authors used DMSNs with a pore size of 14.5 nm and pore volume of 1.39 cm^3g^{-1} (Fig. 8B) and demonstrated that the obtained insulin kit was 2000 times more sensitive than the commercial insulin ELISA kit [22]. In another example, DMSNs containing HRP were functionalized with poly(-amino acid) multilayers (PAMs), which enhanced the ELISA's sensitivity to about 10^4 times higher than the conventional ELISA tests (Fig. 8C) [168]. Liu J. et al. constructed efficient chlorpyrifos (a widespread chemical compound generally used to extinguish insects) aptameric biosensor using dendritic fibrous nano-silica (DFNS) particles functionalized with an amino group (NH_2-DFNS) with enhanced sensitivity [166].

Chondroitin sulfate (CS), a natural glycosaminoglycan structure, provides suitable sites for the absorption the specific molecules [167]. CS conjugated with amino-terminated dendritic mesoporous silica nanoparticles (A-DMSNs) can isolate or increase the

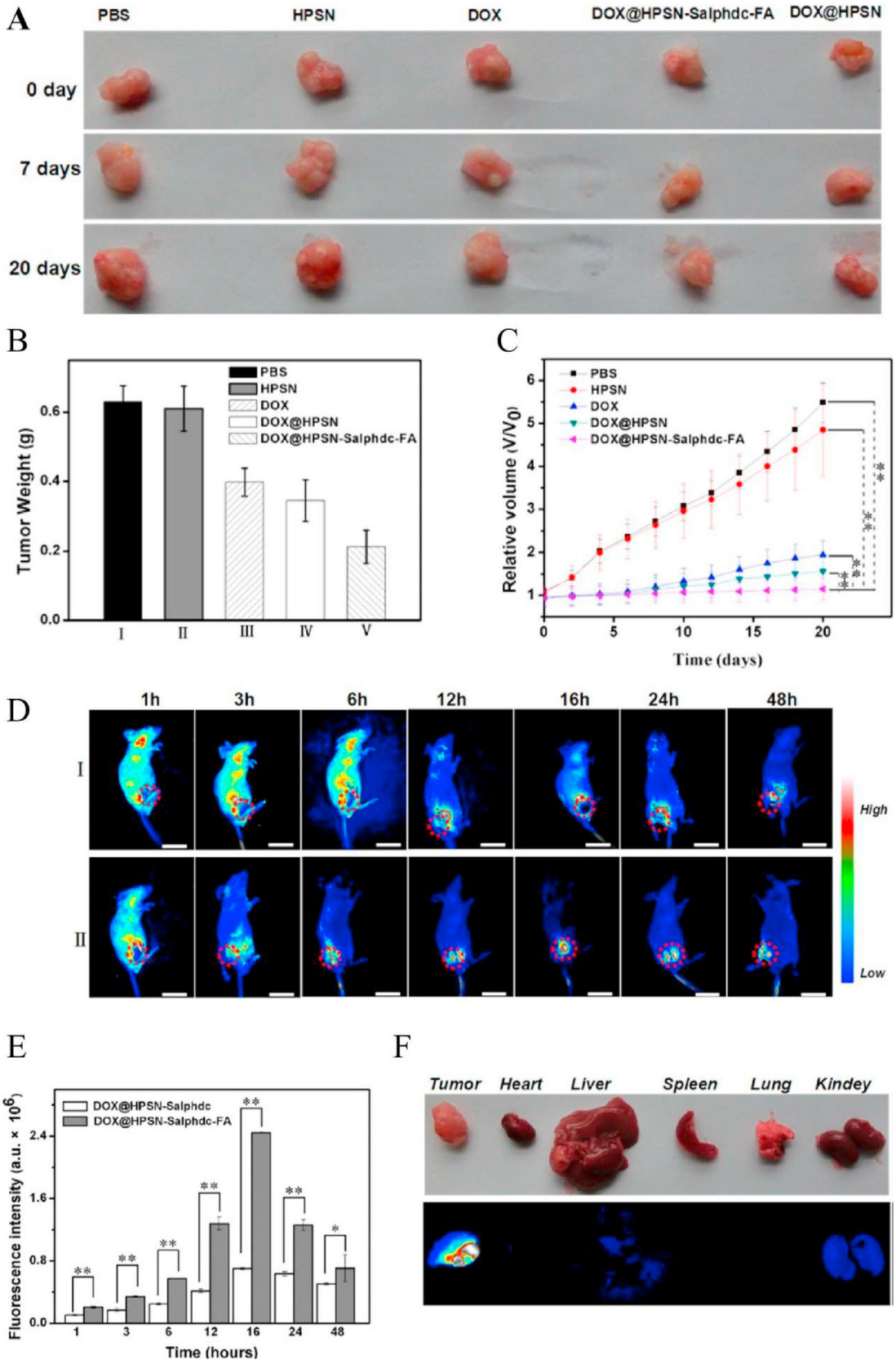

Fig. 7. (A) After treatment, photo images of tumor tissues with PBS (control), HPSNs, DOX, DOX@HPSN, and DOX@HPSN−Salphdc−FA for 0, 7, and 20 days, respectively. (B) Final weights of tumor tissues treated with drug/nanoparticles for 20 days. (C) Relative tumor volumes of nude mice after different treatments. (D) Whole-body real-time fluorescence imaging of DOX@HPSN−Salphdc (I) and DOX@HPSN−Salphdc−FA (II) for 1, 3, 6, 12, 16, 24, and 48 h, respectively. The dash cycles represent the tumor locations. Scale bars: 3 cm. (E) Histogram of the fluorescence intensity of tumors after injection of DOX@HPSN−Salphdc and DOX@HPSN−Salphdc−FA for 1, 3, 6, 12, 16, 24, and 48 h, respectively. (F) Images of main organs (spleen, tumor, kidney, liver, lung, and heart) after injection of DOX@HPSN−Salphdc−FA for 16 h. The error bars indicate that the mean is ±SD (n = 4). (**) It is reproduced from Ref. [164] with permission from the American Chemical Society.

concentration of biological compounds such as proteins since CS composition is similar to low-density lipoprotein receptor (LDLR). Cao et al. conjugated A-DMSNs with CS to absorb low-density lipoproteins (LDL) (Fig. 8D). The proposed method showed excellent efficiency in capturing the LDL from sample matrices, revealing that can separate specific proteins among complex biological samples [167].

In another study, mesoporous structured silica nanofibrous membranes (MPSNMs) were produced to absorb tetracyclines (TCs) from wastewater and sewage. MPSNMs provided high surface area, high porosity with large pore volume fibers with flexible mechanical properties which could be bent easily without being fractured. The authors demonstrated that two main mechanisms, i.e., hydrogen bonding and electrical attraction interactions, participated in TCs absorption, which had a synergic effect on the capacity of MPSNMs to harvest the TCs from aqueous suspensions [169].

Jiahu et al. [170] also produced dendritic fibrous nano-silica (DFNS) nanoparticles anchored with $Nd_2Sn_2O_7$ as an active photocatalyst. The proposed coated NPs demonstrated a great capacity to absorb metronidazole from the aqueous solutions [170].

5. Therapeutic applications of DMSNs

The use of DMSNs for various therapeutic applications such as chemo-, photodynamic- (PDT), photothermal- (PTT), sonodynamic-, chemodynamic- (CDT), and immuno-therapy as well as for the treatment of different infectious or inflammatory diseases and tissue regeneration have been reported. Using DMSNs, it is possible to encapsulate drugs, and biomolecules, and also to engineer drug delivery vehicles that allow a spatiotemporal release of therapeutic cargo while minimizing undesirable toxic effects compared with conventional treatments.

5.1. Utilizing engineered DMSNs for drug delivery in cancer

Several strategies, including surgery, radiotherapy, and chemotherapy, have been employed in clinics for cancer therapy [171], and are widely used. Moreover, several drug-loaded nanoparticles have been reported to target the tumor tissue and generate a therapeutic response. Besides, as we mentioned above, DMSNs are potential platforms with high loading capacity and can be easily designed to respond to external or internal specific stimuli. In the case of cancer, the tumor microenvironment (TME) provides several stimuli that can be used to trigger drug delivery. Moreover, the modulation of TME using nanotechnology has gained attention in recent years [172–174], and it has been found that DMSNs could help cancer therapy by regulating various specific factors in the TME [175]. Hallmarks of the tumor microenvironment (TME) include hypoxia, high interstitial fluid pressure, increased glutathione (GSH) expression, increased concentration of H_2O_2, increased lactate production, expression of vascular endothelial growth factor VEGF, expression of specific receptors like folic acid and CD133, and an increased expression of GLUT (glucose transporter). Typically, DMSNs are loaded with one or a combination of payloads, which can apply via injection either intravenously or directly to the tumor location, with the subsequent DMSNs internalization in cancer cells via endocytosis where the drug is released.

A pH change can trigger cargo release in pH-responsive DMSNs, and several examples using this mechanism have been reported for cancer therapy. Dextran-coated DMSNs loaded with DOX were covalently bonded to a CD133 aptamer to deliver DOX to HT-29 tumor cells. With a pore size in the range of 2–25 nm, the modified DMSN was internalized rapidly, showing an accelerated drug release at pH 5.4. The authors demonstrated that the nanoparticles are helpful to target the overexpressed CD133 receptors on the membrane of the cancer stem cells [99]. In addition to chemical drugs, DMSNs have also been used to design nanozymes by encapsulating small metal ions within their porous structure to induce cancer cell death and regression of solid tumors [16]. In another work, the authors developed cyclometallated gold complex-containing DMSNs functionalized with folic acid as targeting ligand. The work demonstrated that DMSNs were taken up by MCF-7 cells via receptor-mediated endocytosis. Moreover, the release of the cyclometalleted Au complex was reported to be pH-dependent [66]. In another example, Taleghani et al. loaded the iron-chelating agent Deferasirox on DMSNs to reduce high concentrations of iron in cancer cells. Li et al. prepared the nanocomposite FeOCl@H-DMOS-AA/PEG based on hollow dendritimesoporousus organosilicon (H-DMOS) loaded with iron oxychloride (FeOCl), ascorbic acid (AA), and coated with poly (ethylene glycol) (PEG) [107] and found that the nanocomposite produced high levels of toxic hydroxyl radicals even at pH 7. The system was very effective in eliminating the tumor in a mice model.

Another interesting approach to induce cytotoxicity in the TME using DMSNs involves the delivery of enzymes for depleting lactate in tumors. Tumor cells uptake glucose via aerobic glycolysis and produce lactate in large volumes. The produced lactate regulates angiogenesis, tumor invasion, and metastasis due to acidification of the TME. Lactate oxidase (LOX) is an 80 kD enzyme specialized in oxidizing lactate to pyruvate and hydrogen peroxide [176]. Due to the high concentration of lactate in tumors (10–40 mM) [177], high amounts of LOX are needed for efficient lactate depletion. Depletion of LOX has two consequences in tumor biology (1) anti-angiogenesis and anti-metastasis effects following the down-regulation of VEGF and (2) generation of cytotoxic H_2O_2 and raised hypoxia. Besides hypoxia has been used to activate hypoxia-responsive prodrugs such as AQ4N (or banoxantrone) [178]. Due to the high toxicity of high LOX doses, Tang et al. developed innovative openwork@dendritic mesoporous silica NPs (ODMSN) for LOX and AQ4N delivery to the TME. The synthesized ODMSNs showed a particle size of 176 nm. These NPs have a large pore diameter (~27 nm), high surface area (~9 16 $m^2\ g^{-1}$), and pore volume (~4.02 $cm^3\ g^{-1}$), making ODMSN an excellent carrier for LOX with a high loading capacity (~731.8 ± 15 μg mg^{-1}) [178]. The DMSNs developed delivered LOX to the tumor and were able to catalyze lactate oxidation to pyruvate and H_2O_2 in mice *in vivo*. The nanoparticles decreased the lactate concentration by more than 95%, generating cytotoxic H_2O_2, elevating hypoxia, and activating the co-delivered prodrug AQ4N (Fig. 9A, i). This combinatorial treatment of DMSN + LOX + AQ4N achieved a 100% survival rate in mice. The combination of DMSN + LOX + AQ4N enhanced tumor hypoxia (Fig. 9A, ii) and a reduction in angiogenesis and VEGF expression (Fig. 9A–iii). These effects remained for 72 h, which delayed the tumor growth from 6 to 9 days, while the direct administration of LOX resulted in a high death rate of ince [179].

Fan et al. reported the use of the combination of NO and cisplatin, and wrinkled mesoporous silica NP (AMS) to eliminate NSCLC cells. Nitric oxide (NO) is one of the well-known physiological messenger agents which plays an important role in angiogenesis, immune responses, apoptosis, and cardiovascular homeostasis [68,181,182]. However, a drawback of NO molecules is their poor stability and very restricted half-life [183–185]. In cancer treatment, NO efficiently kills cancer cells through the oxidation or nitrosation of mitochondria and DNA. Interestingly, NO can sensitize cancer cells to cisplatin. The authors demonstrated that adsorbed cisplatin on amine-functionalized N-diazeniumdiolate (as NO donors) AMS induced the eradication of NSCLC cell lines [186].

Photodynamic therapy (PDT) combines light energy and a photosensitizer to generate reactive oxygen species (ROS) to kill

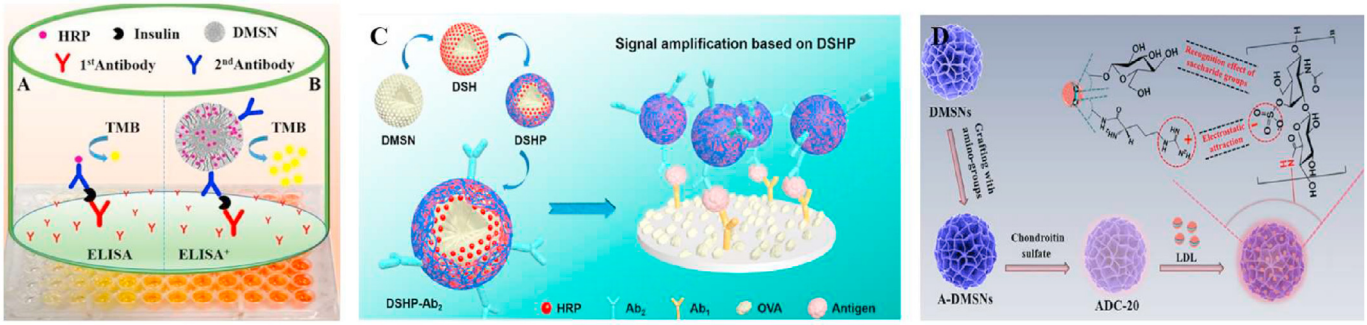

Fig. 8. Application of DMSNs in sensing the biological molecules. (A) Conventional ELISA testing method. (B) DMSNs encapsulated HRP was used in a similar ELISA, which resulted in higher sensitivity of the Insulin detection [22]. (C) DMSNs loaded HRP modified with poly(amino acid) multilayers were applied to increase the sensitivity and stability of the ELISA system [168]. (D) The amino-terminated dendritic mesoporous silica nanoparticles (A-DMSNs) functionalized with chondroitin sulfate (CS) were structured to capture the LDL [167].

cells [187]. More than one type of ROS can work in synergy, and for instance *OH is used along with $^1O_2$ to damage bioorganic molecules, including DNA, lipids, and proteins. For PDT, lasers and non-coherent light sources have been used [188]. This process can be employed in combination with a mechanism that feeds O_2 to the tumor, for instance, using catalysts that can break down compounds to generate O_2. For example, multifunctional DMSNs have been developed using silica doped with fullerene C60 as photosensitizers and fluorescent agents for imaging, combined with the loading of the hydrophobic C18 and anti-pAkt mAb as therapeutic cargo. Besides, the fullerene in the silica core was used to generate single oxygen ($^1O_2$) [57]. In a similar study, the combination of an antibody against AKT serine/threonine kinase 1 (mAb anti-pAkt), related to cell survival, and PDT significantly reduced Bcl-2 protein levels compared to each treatment alone. Furthermore, the growing up of DMNSs on the C60 core gives two important features to the synthesized composites, including fluorescent intracellular tracking and significant inhibition of cell viability [57]. In another study, Ce6 photosensitizer-loaded Pt-decorated DMSNs functionalized by a mitochondrion targeting ligand were successfully developed for improving PDT therapeutic effect in A549 lung cancer cells. As the presence of O_2 is an essential pre-requisite for enhancing the PDT efficacy, in this work, targeting mitochondria by nanoparticles that had catalytic activity for producing H_2O_2 was used to tackle the tumor hypoxic microenvironment [57].

A sustainable ROS generator was developed by Liu et al. for anti-tumor therapy. The internal pores of hyaluronic acid (HA)-DMSNs (pore size 20 nm) were loaded with Mn_3O_4–Ce6 (MC) particles and tested *in vitro* on the murine breast cancer 4T1 cell line. The rationale behind the encapsulation was the high concentration of HAase in the tumor. The HA layer was digested by the enzyme HAase causing a release of MC particles in the tumor vicinity. The tumor cells then internalized the MCs and degraded them by GSH to release Mn^{2+} ions and the photoinitiator, Ce6. Ultimately, the irradiation of Ce6 produced $^1O_2$ species. Moreover, the Mn^{2+} ions converted H_2O_2 to *OH [189]. Besides, multi-functional nanoplatforms using DMSNs and up-conversion NPs for MRI and CT scan-guided PDT was developed by Liu et al. The authors synthesized DMSNs with a mesoporous silica coating to increase the loading capacity of copper peroxide nanodots, Ce6, and polyethylene glycol (PEG) into the silica pores. The primary function of DMSNs was to enhance NO generation and Cu^{2+} release in TME, while lanthanide ions in UPCN imparted luminescence for imaging [108]. (See Fig. 9B).

Photothermal therapy (PTT) induces cell apoptosis by increasing local heat generation by exposing heat-generating materials to near-infrared radiation (NIR) [190]. PTT is a localized treatment for solid tumors using nanoparticles. Its efficiency is tied to the accumulation of targeted therapeutic nanoparticles, the intensity of the light stimulus, and the light-heat conversion efficiency. The accumulation of nanoparticles in the target site is key to the effectiveness of PTT. Liu et al. engineered manganese-based DMSNs ($DMMnSiO_3$) loaded with indocyanine green (ICG) and glucose oxidase (GOD). The authors demonstrated that the nanoparticles quickly disintegrated in tumor cells due to the presence of glutathione (GSH) and mildly acidic conditions, effectively releasing Mn^{2+}, GOD, and ICG. Mn^{2+} was released from the nanocomposite in a uniform and sustainable manner and acted as a catalyst in oxygen generation from intratumoral hydrogen peroxide. Moreover, GOD was used to consume glucose and generate H_2O_2 and ICG produces PTT upon irradiation at 808 nm. A similar approach was followed by Huang et al. [180] using DMSN loaded with Catalase and ICG, under multimodal ultrasound/photoacoustic image-guided tumor photodynamic therapy. Catalase enzyme in the nanostructure helps in the decomposition of H_2O_2 to produce O_2 for the tumor, which is crucial for enhancing the PTT therapeutic efficiency (producing ROS for cancer cell killing) that was effective by the presence of ICG and irradiation at 808 nm [180]. (Fig. 9C). In another study, the targeting efficiency of DMSNs was increased by coating their surface with cell membranes. These biomimetically camouflaged NPs demonstrate superior properties in blocking the premature release of drugs loaded into NPs and improving the binding to cancer cells due to self-identification, leading to longer blood circulation times [191]. In a similar study, red blood cell membrane camouflaged DMSNs imparted additional stability to the DMSN NPs. The DMSNs were then co-loaded with copper sulfide to improve photothermal and radio-sensitization properties for anti-tumor efficacy [192]. In another study, DMSNs with leukocyte/platelet hybrid membrane co-loaded with doxorubicin and a NIR fluorescent dye showed an improved targeted efficiency towards triple-negative breast cancer. The average pore diameter of 9.0 nm led to a large drug loading capacity (T. Znag et al., 2021). Li et al. embedded oil-soluble Ag_2S QD crystals, as NIR responsive nanoparticles, in 60 nm DMSN with doxorubicin-loaded in the DMSN pores [193].

Overall, DMSNs with a good dispersity and spherical, uniformly-dendritic morphology have efficiently been used in a synergistic approach by combining PTT and PDT modality to enable a catalyst-driven cascade mechanism [106]. The properties of DMSNs can be further enhanced by integrating a functional host within the nano platform to provide distinct properties. For example, graphene nanosheets used as a host within the DMSNs improved biocompatibility, biodegradability, surface area, and drug loading capacity. Upon conjugation of curcumin-loaded, graphene oxide integrated

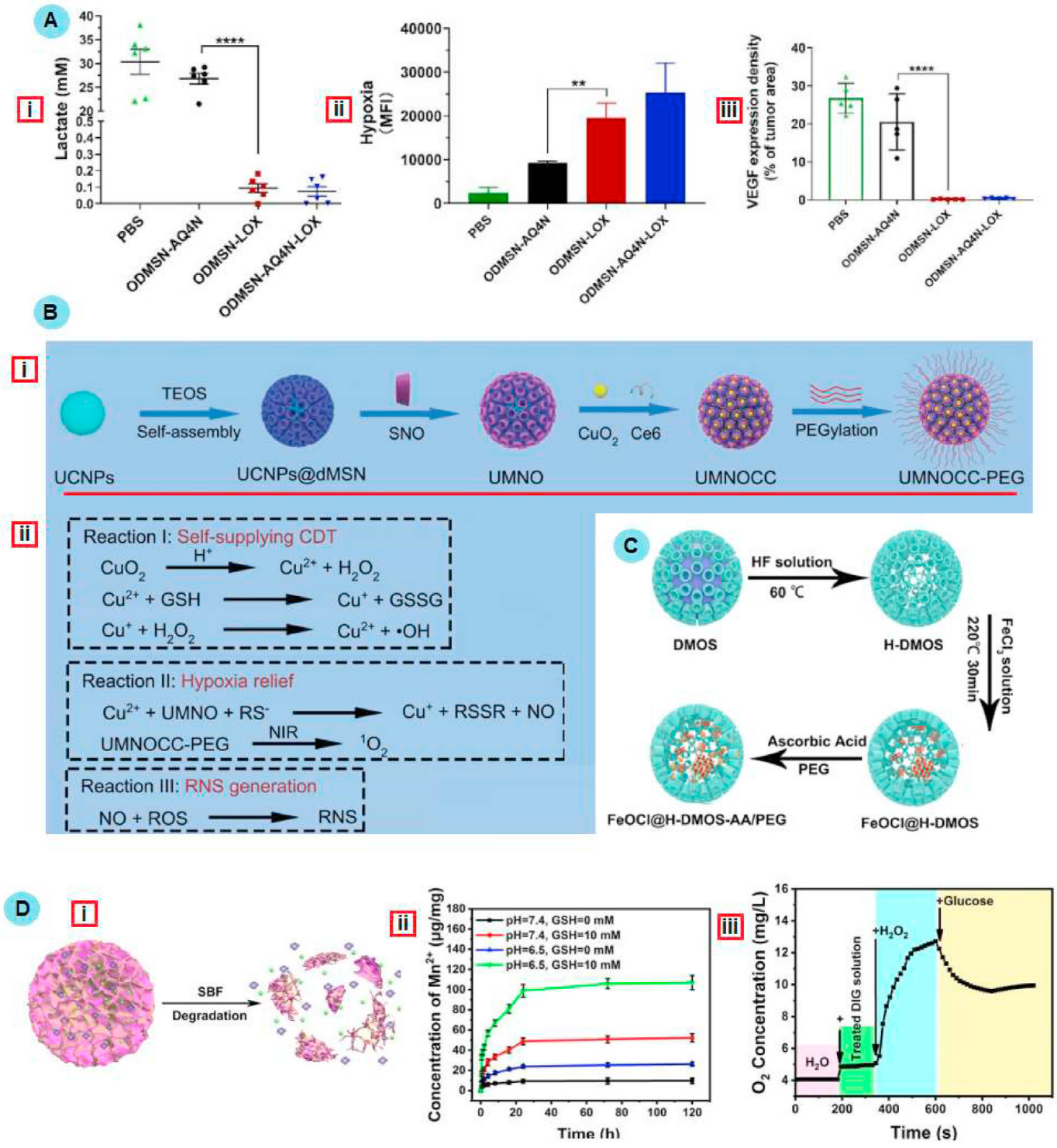

Fig. 9. A) (i) changes in the concentration of Lactate in the 4T1 tumors model after 48 h of DMSN injection. (ii) hypoxia level under different treatments, (iii) VEGF level based on stained area for tumor sections [178]. B) (i) the UMNOCC-PEG synthesis illustration, (ii) the therapeutic mechanism introduced for UMNOCC-PEG to improve PDT induced by gas therapy, Cu^{2+}-initiated chemodynamic therapy, and NIR [108]. C) The synthesis process of FeOCl@H-DMOS-AA/PEG [107]. D) the (i) biodegradation process of DMMnSiO3 NPs loaded with ICG and GOD, (ii) the concentrations of released Mn^{2+} in TME at different times, (iii) dissolved oxygen concentration in TME [180].

DMSNs with folate; a PTT platform was established to release curcumin to induce cell apoptosis. Similarly, gold NPs were immobilized in the DMSNs as PTT agents [194]. All these examples demonstrated the potential of DMSNs, due to the controllable pore sizes, wide specific surface area, unique structures, biodegradability, good biocompatibility compared to typical NPs, and high loading capacity to deliver multi-therapeutic agents for TME modulation in drug-based and enzyme-based therapy.

Sonodynamic therapy (SDT) encompasses non-thermal therapeutic ultrasound applications. The mechanism behind the working of SDT is not yet fully understood. However, the ultrasonic cavitation effect is a possible contributing factor to the efficacy of

SDT [195,196]. As a result of this cavitation effect, sonoporation occurs. This causes transient micropores that ease the vascular permeability of drugs and improve their transport across the cell membrane [196]. The SDT can also induce cancer cell apoptosis via the regulation of gene expression and angiogenesis. Sonosensitizers in a drug-delivery platform used in SDT get excited upon ultrasound irradiation and release energy upon returning to the ground state. The molecular O_2 absorbs this released energy to generate ROS. Different sonosensitizers like TiO_2 offer good thermal and photostability along with excellent biocompatibility. Although SDT cannot be used as a stand-alone therapy to eliminate tumor cells, it can increase cytotoxicity by enhancing the uptake and release of drugs. For example, the therapeutic efficiency of polyethyleneimine-folic acid-coated DMSNs loaded with curcumin used in SDT showed encouraging results as an anticancer platform. Folic acid was used as a targeting ligand and was linked to the DMSNs via polyethyleneimine. Curcumin was loaded onto the DMSNs as an anticancer drug. Curcumin was released in a controlled manner, and its release rate depended on the ultrasound irradiation time. When the DMSNs were tested on the HeLa and A549 cells, excellent anticancer activity was observed [86]. In another study, Zuo et al. designed DMSNs containing ultrasmall $Cu_{2-X}S$ NPs and Rose Bengal (sonosensitizer). These DMSNs were used to target oral squamous cell carcinoma (OSCC). When irradiated with both NIR laser and ultrasound, OSCC cell death was induced. Furthermore, the intravenous administration of these DMSNs into mice showed satisfactory biocompatibility and biodistribution at the tumor sites [197].

Chemodynamic therapy (CDT) produces *OH radicals from H_2O_2 via Fenton and Fenton-like reactions [198]. The CDT leverages the overproduction of H_2O_2 to produce free radicals that induce cytotoxicity in cancer cells. The NPs utilized in CDT usually incorporate enzymes or inorganic particles that catalyze the reduction of H_2O_2. A continuous supply of H_2O_2 is necessary for a successful CDT. For this purpose, DMSNs have been used as large-pore supports to encapsulate bulky enzymes and nanoparticles. A large-pore DMSN support incorporating Fe_3O_4 NPs set up sequential catalytic reactions to liberate *OH radicals. The large pore size (40 nm) of the DMSN platform also contained glucose oxidase enzyme to maintain a supply of H_2O_2 [199]. Besides, Li et al. recently developed a hollow DMSN system, confining FeOCl NPs within the silica structure. In this study, ascorbic acid was used as a prodrug for the generation of H_2O_2. It was shown that ascorbic acid in the extracellular environment in the presence of serum could produce ascorbate radicals, and subsequently, these radicals produce H_2O_2 which finally promotes cancer cell death. Further, this system also showed effective metastasis inhibition and enabled T_2-weighted MRI capability [107]. Li et al. designed a nanozyme formulation by co-loading CaO_2 and Fe_3O_4 NPs within a pH-sensitive DMSN construct. Following intravenous injection in mice, DMSNs released the NPs within the weakly acidic media in TME. The released CaO_2 reacted with the H^+ ions to produce H_2O_2 that then underwent a Fenton reaction with Fe_3O_4 to produce toxic *OH radicals. An efficient synergistic mechanism inducing ferroptosis and immunomodulation occurs [18]. Like PDT, CDT can also be combined with other therapies such as PDT and PTT for increased treatment efficacy [200]. Dong et al. coated uniformly sized down conversion NPs with DMSNs and then loaded them with ultrasmall oxygen-deficient molybdenum oxide NPs. In vitro tests showed that HeLa cells efficiently internalized the DMSNs, resulting in reduced survival of the cells. Moreover, the nanoparticles were used for PTT and CDT therapy in an *in vivo* model [201].

Immunotherapy for cancer treatment has been raised as an alternative strategy to conventional treatments by stimulating the immune system for cancer cell killing. Besides, in recent years, nanomaterial-based immunotherapy has shown promising to potentiate the efficacy of cancer immunotherapy and reduce side effects. Different NPs can be used to deliver cancer antigens and therapeutic drugs to cancer cells. In addition to the medicinal cocktail, NPs are often modified to carry adjuvants that enhance treatment efficacy. Xing et al. synthesized dendritic porous silica nanoparticles (DPSNs) modified with aminopropyl groups and loaded with bovine serum albumin (BSA). The NPs achieved an efficient loading of BSA protein and provided a versatile method of synthesizing DPSNs with tunable asymmetric features [202]. Shi et al. reported a light-traceable, intracellular microenvironment-responsive drug delivery system that was synthesized using a combination of DMSNs, gold NPs, and autofluorescent nanogels. This carrier was loaded with sulfhydryl-containing drug (Captopril). The drug delivery system achieved low cytotoxicity, efficient transport ability, and microenvironment-responsive drug release [203]. However, considering the size of most adjuvants and immunotherapeutics (such as proteins and cytokines), the mesoporous structure and the size of NPs is a crucial factor. This size-related constraint paves the way for DMSNs due to their relatively small particle size and large pore size. Among the different strategies, cancer vaccination is the most widely applied for cancer immunotherapy, and DMSNs have attracted significant attention for vaccine development due to their properties. NPs can be applied as carriers for vaccines and adjuvants to boost immune response [204–206]. Immunomodulatory agents or immunogens are the main parts of an NPs-based vaccine, containing antigens, DNA vaccines, and siRNA [207,208]. These substances can be encapsulated (within NPs lumen, pores, or cavities), conjugated (via covalent linkages), or adsorbed (on the surface of the NPs) [209]. Moreover, immunostimulatory and targeting ligands, such as tissue and immune-specific ligands, and pathogen-associated molecular patterns (PAMPs) can be incorporated into the NPs-based vaccine to target specific cell tissues and elicit inflammatory responses. [210–212]. It is documented that the intended vaccine needs drainage to lymph nodes, internalization by dendritic cells (DC), maturating DCs, and proceeding and presenting MHC I-antigen complexes to CD^{8+} T cells (Scheme 2) [213,214]. In this cascade, the critical step is the internalization of antigen-loaded NPs into DCs; otherwise, the drained NPs leave the lymph node through the subcapsular sinus and the efferent lymph vessel [213,215]. Moreover, it was shown that NPs with a size range of 10–100 nm could pass through the lymphatic endothelial cell gaps and drain into the lymph nodes [216–218] (see Scheme 3).

Biocompatibility, tunable size, easy surface functionalization, ultrahigh specific surface area, and adjustable pore size and chemistry make DMSNs suitable for vaccine delivery applications. Moreover, negative surface charge and hydrophilic surface due to silanol groups (Si–OH) make DMSNs potential lymph node-targeted carriers [71,219]. Several studies utilized DMSNs for vaccine development. Hong et al. [213] synthesized 80-nm DMSNs with different pore sizes loaded with ovalbumin (OVA) antigen to assess the effect of pore size on the mediated-immune responses. The authors labeled OVA with Cy5 (cyanine5) dye to track the derange of DMSNs from the administration site to lymph nodes *in vivo* and their internalization efficiency in DC2.4 cells. They observed that subcutaneously injected Cy5-OVA@DMSNs accumulated into popliteal lymph nodes 10 h after injection (Fig. 10).

In another study, Jambhrunkar et al. [220] synthesized an immunoadjuvant and co-delivery platform based on benzene-bridged mesoporous organosilica NPs for delivery of both antigens (OVA) and toll-like receptor-9 agonists (cytosine-phosphodiester-guanine oligodeoxynucleotide(CpG)). The authors reported that the incorporation of the bridged organosilica framework

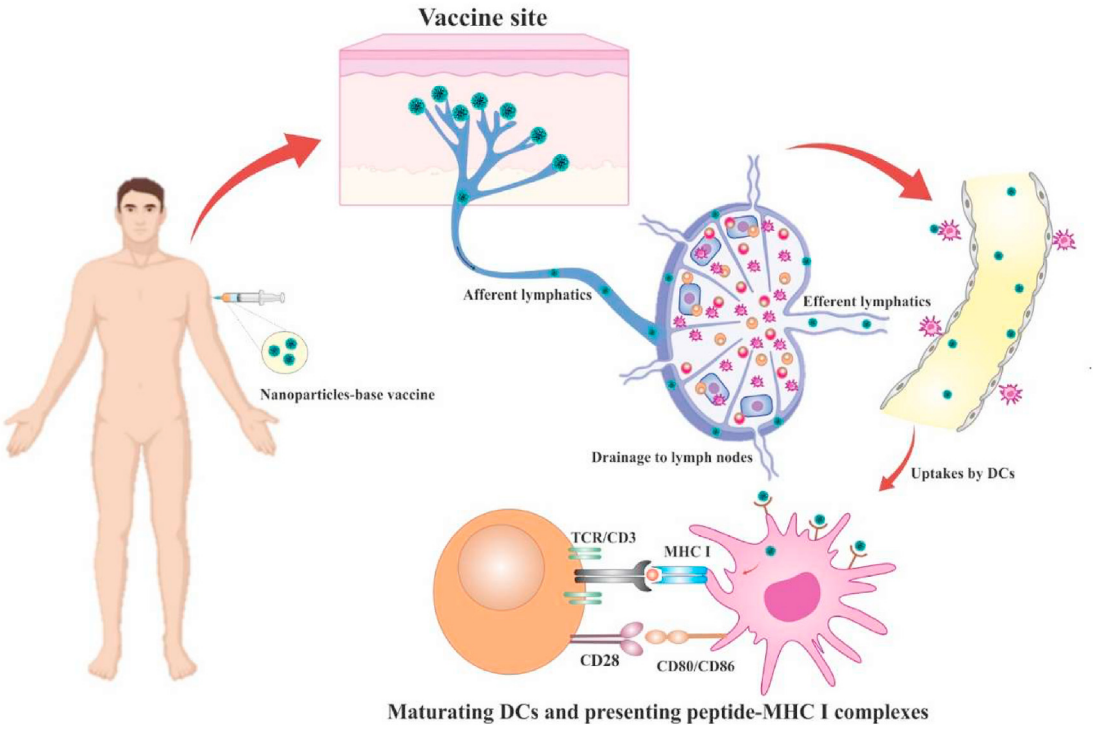

Scheme 2. Schematic representation of the adaptive immune response induced by antigen-loaded lymph node–targeting NPs.

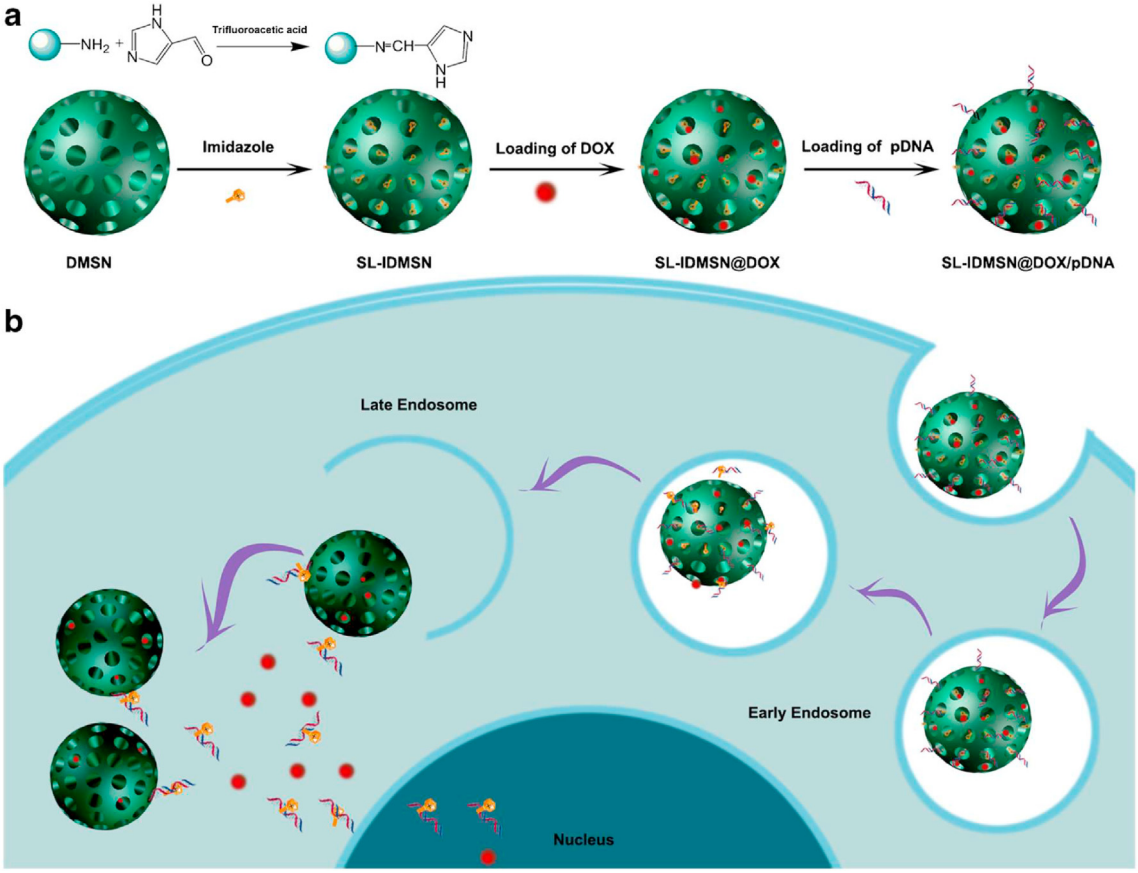

Scheme 3. (a) A schematic illustration of the preparation and drug loading of SL-IDMSN. (b) Intracellular drug delivery by microenvironment sensitive SL-IDMSN [69].

showed a significant effect on the physicochemical properties of NPs. The results indicated that the incorporation of benzene bridge groups resulted in high pore volumes and large pores, with subsequent effective OVA and CpG delivery to DCs. The animal studies showed significant tumor inhibition with 100% tumor-free mice in 25 days.

Cha et al. [219] synthesized a prophylactic cancer vaccine based on extra-large pore DMSNs loaded with OVA and CpG to stimulate antigen-specific cytotoxic T lymphocytes (CTLs). The results showed promoted antigen presentation and stimulation of DCs and enhanced pro-inflammatory cytokines secretion. Animal studies revealed draining lymph nodes targeting the DMSNs, stimulation of CTLs, and significant tumor growth suppression. Another study synthesized extra-large pore DMSNs coated with PEI polymer to endow adjuvant immune properties and modified the NPs surface charge to improve loading and slow release of OVA [221]. The results showed promoted activation of the DCs, the CTLs, tumor growth suppression, and enhanced survival rate. Abbaraju et al. synthesized asymmetric DMSNs with tunable head−tail structures for vaccination and immunotherapy. The authors reported that the structure of the head is adjustable (porous or solid), whereas tail features (tail coverage on head and tail length) are tunable by varying the TEOS volume and reaction condition (Fig. 11). The results showed that the synthesized asymmetric DMSNs exhibited excellent biocompatibility and hemocompatibility. Moreover, uptake and maturation induction of immune cells (macrophage and DCs) through the synthesized asymmetric DMSNs was higher than when using Stöber spheres NPs [222].

In addition, previous research has shown that reactive oxygen species (ROS) could serve as an essential stimulator of immune responses [223,224]. These molecules can prompt the stimulation of dendritic cells (DCs) [225,226] by an increase of CD86 and CD80 for enhancing antigen presentation [227]. In this regard, organosilica dendritic NPs with tetra-sulfide bond structure and functionalized with polyethyleneimine (PEI), are able to GSH-depletion, ROS generation capability, and ability to co-deliver ovalbumin/cytosine-phosphorothioate-guanine (CpG) to immune systems were developed. Neutralizing intracellular GSH levels with tetrasulfide bonds caused increased ROS levels. Also, after being delivered into APCs the is a release of antigen and agonist triggered by the disintegration of nanocomposites in response to cytosolic high GSH concentration (2−10 mM). Afterward, T cell (CD8þ) mediated tumor cell death occurred [71].

As mentioned earlier, crosstalk between cancer cells and other cells located in the TME causes the release of specific biochemical agents that strongly paralyzes the tumor resident immune cells in TME [228,229]. For example, immature myeloid-derived suppressor cells (MDSCs) release suppressive factors to inactivate T cells in response to the abovementioned biochemical agents in the TME [230,231]. So, a new therapeutic paradigm and novel strategies are necessary to activate TME resident immune cells or infiltrate external immune cells into the TME [232]. In recent years, the combination of chemotherapeutic agents accompanied by immunostimulatory agents has been introduced as a new strategy. In this aspect, the exposure to a certain cytokine mixture can act as an activating signal, for the maturation of DCs from monocytes [219]. DCs, after the uptake of extracellular antigens, become mature and present major histocompatibility complex (MHC) type I their its surface. The antigen processing DCs travel to lymph nodes and stimulate the cytotoxic T lymphocytes (CTLs) through the MHC-I complex and T-cell receptors [233,234]. Given that most immunostimulatory agents are macromolecules, the usage of DMNSs for this purpose is a great opportunity while undesired side effects are minimized. For example, TNF-α is an essential protein mediator in cell survival, inflammation, apoptosis, and immunity [235] that cannot be utilized systemically due to its highly toxic effects [236]. It was shown that activation of dendritic cells (DCs) by TNF-α causes immune system-dependent antitumor effects. However, high amounts of this drug (more than 1 mg) are needed to achieve the desired antitumor activity. The administration of this dosage systemically is impossible due to cytotoxic effects, and only local use of this cytokine in melanomas, sarcomas, and unresectable tumis are approved [237]. DMSNs, have been used for encapsulation and shielding of a highly toxic TNF-α homotrimer agonist (Beromun) in combination with a pH-sensitive hyperbranched polyethyleneimine (PEI)-polyethyleneglycol (PEG) copolymer [53]. In another example, extra-large pore mesoporous silica NP (~20−30 nm) has been developed with high efficiency for IL-4 delivery [238].

Following chemoimmunotherapy, a lipid-coated biodegradable hollow mesoporous silica nanoparticle containing two chemotherapy drugs (all-trans retinoic acid (ATRA) and doxorubicin (DOX)) and the immune system regulator interleukin-2 (IL-2) was developed for stimulating tumor immunity (Fig. 12A). The biodegradable and hollow mesoporous silica nanoparticles (BHMNS) depicted high encapsulation capacity and excellent stability, with low systemic toxicity. The sustained drug release behavior of BHMNSs changed the cold immunity atmosphere of TME to a hot environment via stimulation of T lymphocytes and natural killer cells [239]. The remodeling of the TME immune system is changed by the up-regulation of IFN-γ and IL-12 and the down-regulation of IL-10 and TGF-β [56]. Furthermore, nanozyme Pt NPs were deposited on the surface of the channels of DMSNs to catalyze the intracellular H_2O_2 conversion to oxygen. Based on the results, DMSNs could: i) carry a high amount of drugs due to their high capacity, ii) enhance the catalytic activity and oxygen generation (by decomposing the hydrogen peroxide inside the cell), iii) increase the death rate of cancer cells compared to the direct use of drugs (Fig. 12B) [56,163,240].

DMSNs also demonstrated their potential to stimulate T cells and TAM (tumor-associated macrophage) to promote tumor suppression. For instance, Chen and his colleagues synthesized DMSNs loaded with iron oxide for cytotoxic T cell activation and macrophage polarization (Fig. 12C, i) [240]. $CD80^+$ and $CD86^+$ B cells, as M1 markers, experienced higher activation and approximately 3−4 times upregulation to show antitumor effects. Due to iron oxide, this activation was higher in DMSNs-based treatments than in the current treatments (Fig. 12C, ii). The weight of the tumors was measured after implantation (injections of vaccine for female C57/BL6 mice), and the results showed that employing DMSNs caused a significant reduction in the weight of tumors (Fig. 12C, iii). The principal reason was ascribed to the high loading potential of the DMSNs.

Combinatorial cancer therapy can also be envisioned using DMSNs involving PTT/starvation therapy/immunotherapy. In a study by Li et al., the DMSN platform was co-loaded with Au NPs and Imiquimod (R837), an immunostimulator. DMSNs were coated with a pH-sensitive cell membrane to facilitate the loading of R837. *In vitro*, cellular uptake results showed that DMSNs were efficiently taken up by the 4T1 cells. Furthermore, *in vivo* results on mice showed a synergistic effect of PTT/starvation therapy/immunotherapy on the tumor via tumor ablation. The study demonstrated that the use of R837 along with Au NPs loaded on DMSNs generated a vaccine-like function by inducing a long-term memory effect for inhibiting tumors [17].

5.2. Gene therapy

Human gene therapy (GT) is rapidly gaining popularity due to the development of novel gene carriers [241−244]. The advent of

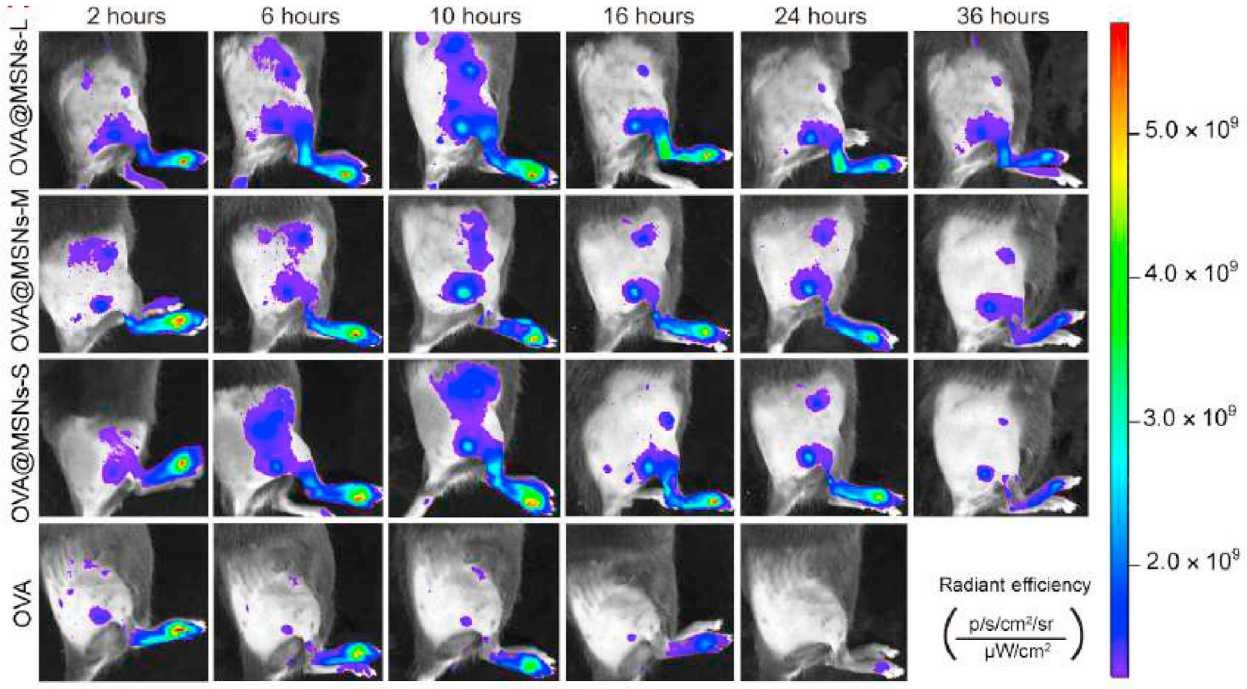

Fig. 10. The DMSNs derange from the administration site to lymph nodes *in vivo* imaging using an IVIS Spectrum system. p, photon. Reproduced with permission from [213].

adenoviral vectors and lentiviral vectors enables GTs for acquired and inherited genetic disorders. Currently, silica NPs-based GT suffers from low efficiency of passive-diffusion release of DNA and RNA due to strong electrostatic interactions between negatively charged genes and positively charged NP surface. This problem provides a clear rationale for utilizing large-pore DMSNs for loading genetic content. In a traceable gene delivery platform, DMSNs were loaded with 30 μg plasmid DNA (pDNA) per mg of NPs. To avoid electrostatic interactions and increase gene transfection efficiency, the DMSN surface was functionalized with an acetaldehyde-

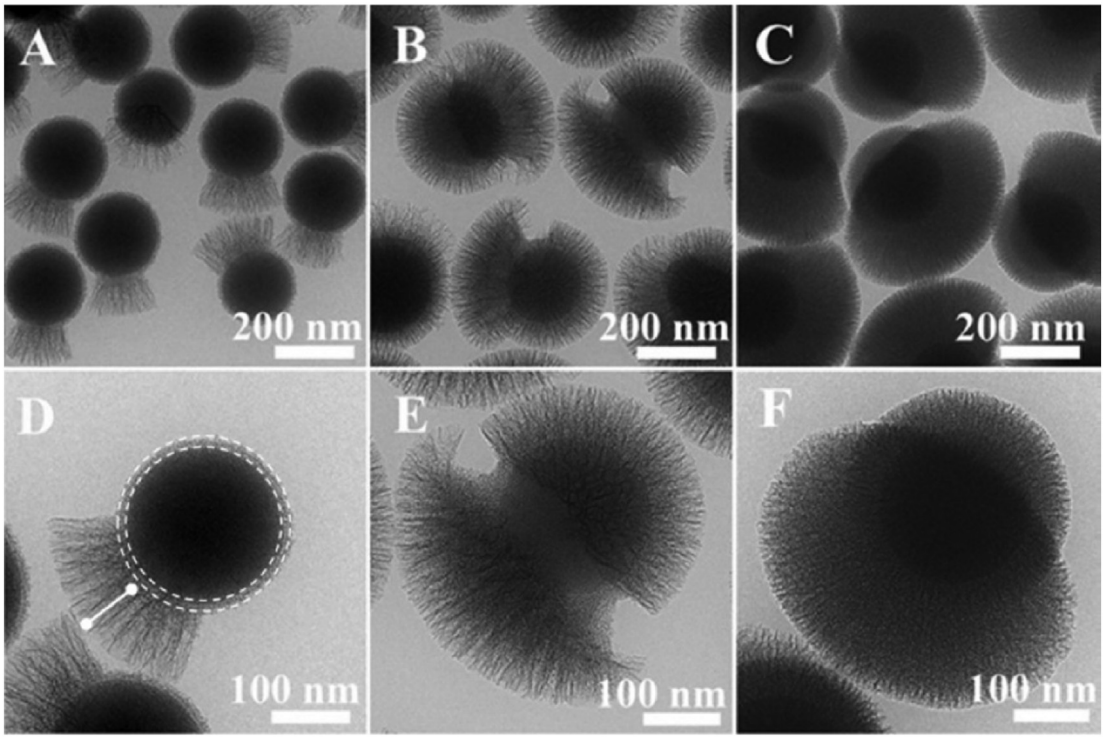

Fig. 11. TEM images of DMSNs prepared at varied TEOS volume V. (A and D) V = 0.41 mL, (B and E) 1.25 mL, and (C and F) 3.75 mL. Reproduced from Ref. [222] with permission from the American Chemical Society.

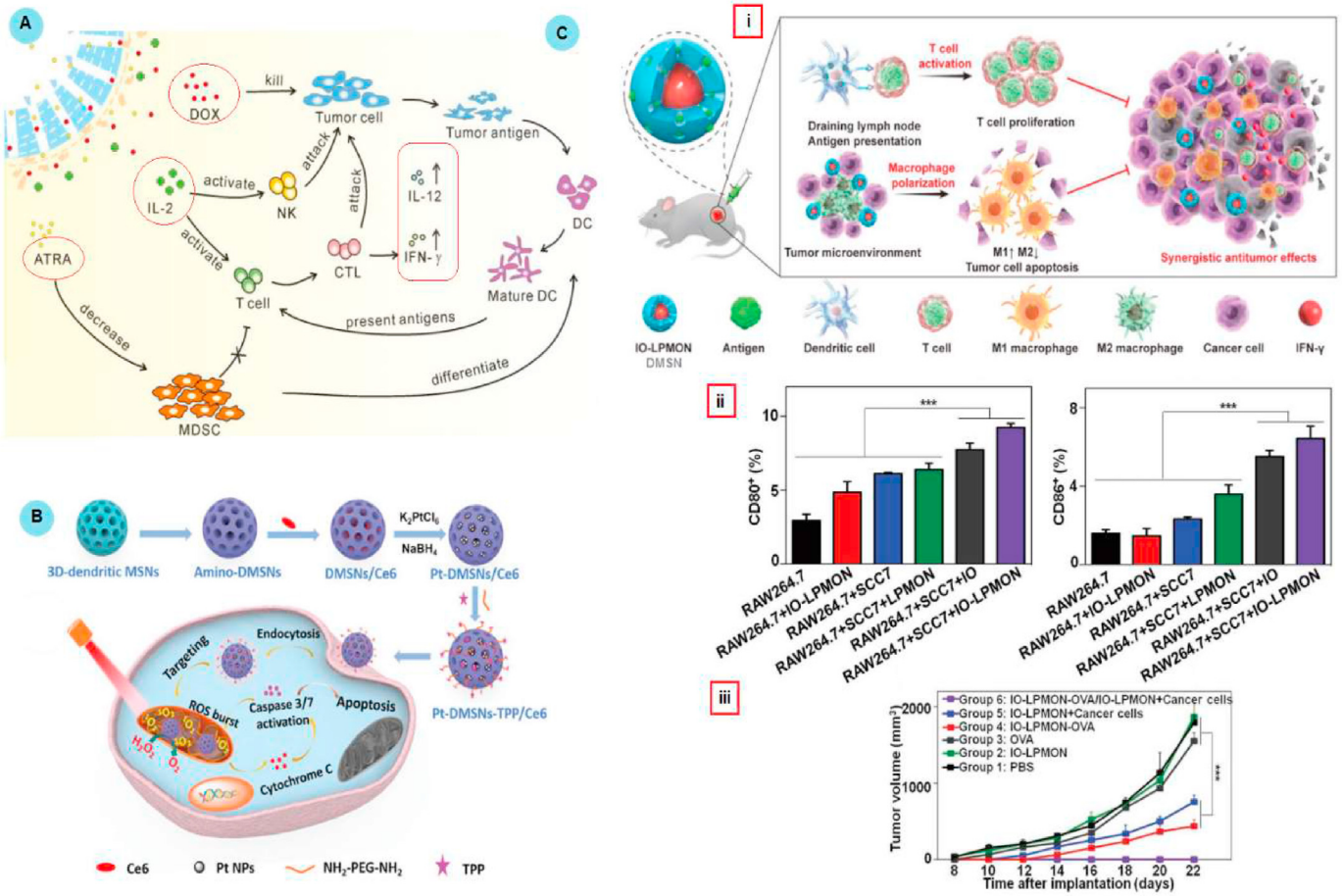

Fig. 12. A) BHMSNs could release all three factors to kill cancer cells and regulate TME [56]. B) synthesis of DMSNs-based NPs and how they enhance PDT. C) (i) T cell activation and polarization of macrophages occur by DMSNs (IO-LPMONs) as significant antitumor immunotherapy [163]. (ii) Expression of CD86 and CD80 in the co-culture systems under different treatments, (iii) Tumor volume during in-vivo study under different treatments [240].

modified-cysteine [73]. DMSNs with fibrous structures and large pores (KCC-1) are better suited for transporting DNA and genes due to their effective adsorption property. Genes can be readily adsorbed onto the internal or external surface area of KCC-1 [20].

Simultaneous delivery of a drug and genetic materials is another exciting and promising approach for combating diseases. To address this, an imidazole modified DMSN (SL-IDMSN) was used as a pH-responsive system for delivery of DOX and Survivin shRNA plasmid (iSur-pDNA) [69]. In this system, imidazole rings get a positive charge at acidic pH, which helps to more intense electrostatic condensation of plasmids and protects them from blood endo/exo nucleases. In addition, in the environment of endo/lysosomes, the Schiff-base linker with imidazole is hydrolyzed, allowing plasmid release. Moreover, the proton sponge effect due to imidazole groups allowed endosomal scape and spread of the plasmid into the cytosol.

Polyethyleneimine (PEI) functionalized DMSNs have been also used to co-deliver topotecan and pEGFP-N1 plasmid effectively into HeLa cells [245]. Similar to DNA delivery, mRNA was packaged within a surface-modified DMSN to improve endosomal escape [246]. In another study, DMSNs were integrated with other NPs to improve the co-delivery efficiency of small molecules and genetic materials. For instance, cyclodextrin-modified PAMAM (β-CD PAMAM) dendrimers were used to load various therapeutic agents, including hydrophobic and hydrophilic anticancer small molecule and siRNAs genetic materials [247,248]. Also, DMSN and β-cyclodextrin-modified PAMAM (3.0G) dendrimers were used to deliver both the anticancer small molecule nitrophenyl benzyl carbonate [249,250] and Bcl-2 siRNAs with high efficiency [73].

5.3. Engineered DMSNs in tissue applications

Recently, DMSNs have attracted interest in tissue engineering (TE) applications due to their easy functionalization, high specific surface area, good biocompatibility, tunable pores, and abundant surface chemistry [251–253]. According to our survey, although DMSNs have attracted tissue engineers' attention, only a few studies have been published in the literature, but an increasing trend was observed. Different roles of DMSNs in TE primarily focus on the delivery of bioactive factors, bioactivity, stem cell labeling, and the impact of MSNs on mechanical and physicochemical properties of scaffolds (Nicely reviewed by Chen [254]).

5.3.1. Bone tissue engineering

Previous studies revealed that the release of Si ions from DMSNs incubated with hBMS (human bone marrow stromal) cells promotes osteogenesis. The reason was attributed to the biodegradability of DMSNs which results in Si sustained release. In another study done by Lei et al. [255], a new hydroxyapatite-DMSNs scaffold was fabricated for bone regeneration purposes. The obtained results from gene expression including osteopontin (OPN), osteocalcin (OCN), collagen type I alpha 1 (CoL1A1), runt-related

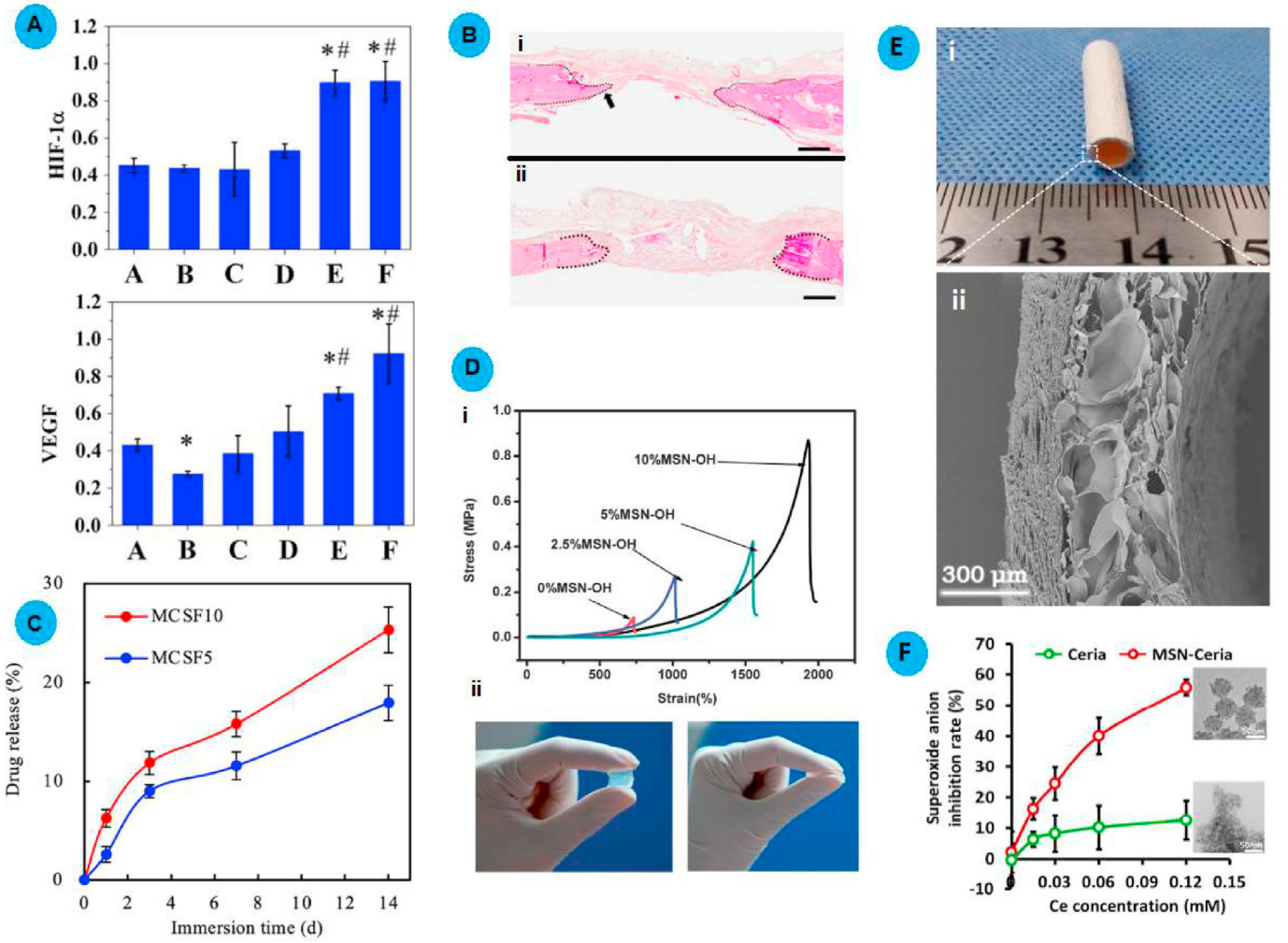

Fig. 13. A) Enhancement in the HIF-1α and VEGF proteins expression due to the release of dimethyloxalylglycine and Si ions from MSNs [272]. B) H&E staining belongs to calvarial defect samples (i) treated with HA-DMSN and (ii) blank control [255]. C) FGF-2 release from DMSN-based scaffolds with 5 and 10% FGF-2, soaked in PBS at 37 °C for 14 days [256]. D) (i) Stress-strain curves for the hydrogel containing various amounts of MSNs-OH (0–2.5–5–10 wt %), and (ii) a qualitative image comparing the compression behavior of both MSN-based (left) hydrogel and the pure one (right) [262]. E) (i) Digital photos, and (ii) Cross-sectional SEM images of the electrospun bi-layered vascular scaffold. F) MSN-Ceria neutralized superoxide anions compared with pure ceria aqueous suspension.

transcription factor 2 (RUNX2), and integrin-binding sialoprotein (IBSP) indicated the improved osteogenic potential of the scaffold. *In vivo* studies showed that the scaffold resulted in more bone formation after four weeks (Fig. 13B). In another research, fibroblast growth factor-2 (FGF-2) was loaded onto mesoporous calcium silicate NPs as DMSN and embedded in a PCL-based scaffold [256]. The authors found that DMSN gradually delivered FGF-2 during scaffold degradation, affecting osteogenesis differentiation and proliferation of HWJMSCs (human Wharton's jelly mesenchymal stem cells) (Fig. 13C).

5.3.2. Scaffold improvement

Apart from employing DMSNs and the scaffold to deliver bioactive factors during tissue regeneration, the presence of DMSNs also showed their effect on scaffold properties. Apart from the technique of scaffold fabrication such as 3D bioprinting and electrospinning, DMSNs showed their potential to positively affecting the mechanical degradation, cell attachment and proliferation, and porosity of the final scaffold [257–260]. Such an improvement was carried out previously using mesoporous silica nanoparticles. For instance, Wang et al. integrated mesoporous silica nanoparticles with a gelatin hydrogel scaffold. They reported that the micropore size and the mechanical behavior of the final scaffold increased [261]. In another research, a novel hierarchical hydrogel made of (poly(ethylene glycol diacrylate)) (PEGDA) and hydroxyl mesoporous silica nanoparticles was developed [262]. The results of the mechanical evaluation confirmed that the stress of breaking of the hydrogel containing 10% mesoporous silica nanoparticles was approximately ten-fold stronger than that of the pure hydrogel (Fig. 9D). Thereby, it can be predicted that DMSN, due to their higher surface area, can depict better efficacy in scaffold improvement. For example, the addition of DMSNs improved the mechanical behavior of hydrogels without affecting permeability or rigidity. It was also shown that a potent interaction occurs between the polymer matrix of polyacrylamide and DMSNs [263]. In another study, DMSNs were embedded in polyethylene glycol dimethacrylate hydrogel to boost biological activity and mechanical behavior. Results revealed that the presence of DMSNs was beneficial to promote elastic modulus, and cell viability and act as biomolecule carriers [264].

5.3.3. Vascular tissue engineering

Other studies reporting the role of DMSNs in TE focused on vascular TE and the angiogenesis activity of DMSNs. DMSNs show their ability to improve revascularization during TE by carrying specific cargoes and anticoagulants [265,266]. Guo and colleagues [265] fabricated an electrospun bi-layered tubular scaffold as an implant for blood vessel TE (Fig. 13E). The implant contained DMSNs that were used as a carrier of salvianolic acid (10%). The authors found that the presence of DMSNs decreased the elastic modulus compared with the DMSN-free scaffold. In a similar study in 2017, Wu et al. [239] used heparin-loaded DMSNs embedded in a silicon substrate to promote anticoagulation. The scaffold containing DMSNs displayed notable blood compatibility, and no blood coagulation or platelet adhesion was observed.

5.3.4. Wound healing

To accelerate the process of wound healing, tissue function recovery, protection against inflammation, and prevention of infections are mandatory [267–269]. DMSNs can be used as a potent growth factor carrier, and in addition, their presence can help cell adhesion. Scientists reported employing DMSNs in wound healing and skin tissue regeneration. For instance, in 2018, Wu and his colleagues first coated ceria NPs on the surface of DMSNs, and the final nanocomposite was directly employed for wound healing [270]. The authors claimed that this nanocomposite could play a vital role as ROS-scavenger. In fact, high adhesion to the tissue and restriction of ROS exacerbation was reported as distinguishing features of the DMSNs-based nanocomposite. Considering inflammation during the wound healing process, Pan and his colleagues also used DMSNs directly to the wound area on the rat's back [271]. Results showed that DMSNs were a versatile and convenient adhesive that helped wound closure and inhibited inflammation. It is hypothesized that embedding the drug-loaded DMSNs in biopolymeric-based wound dressing can promote the rate of wound healing and skin reconstruction due to its potential for sustained release, regulating inflammation, and cell attachment and proliferation.

5.4. Antimicrobial, infection, and anti-inflammatory therapy

The large surface-volume ratio of NPs allows for greater drug loading capacity and better contact with microbe surfaces to develop antimicrobial therapies [273]. Moreover, NPs can increase the accumulation of the delivered antibacterial cargo at the site of the disease while minimizing off-target side effects [274,275]. Wang et al. synthesized dendritic fibrous silica NPs (DFSNs) that imparted antireflective and antibacterial properties in coatings. In this study, DFNs were coated with well-dispersed Ag NPs onto the surface of poly(methyl methacrylate) (PMMA) polymeric glass via organic vapor treatment. The PMMA slide with the nanocoating showed an 80% efficiency in killing bacteria (*Staphylococcus aureus* and *Escherichia coli*) [276]. DMSNs have been used to encapsulate large enzymes that have antimicrobial properties [277]. Also, compared to traditional mesoporous NPs with a smooth surface, DMSNs show a better drug-delivery efficacy due to enhanced adhesion to bacterial cell membranes by their dendritic structure [277]. Wang et al. showed that DMSNs with a pore size of 22 nm loaded with lysozyme show prolonged inhibition towards *E. coli*, in which the lysozyme had a sustained release pattern [277]. Vaccinations for diseases like foot-and-mouth disease can also be formulated using DMSNs [19]. In the study by Liu et al., DMSNs with large center-radial pores were prepared for macromolecular protein loading and delivery. The DMSNs were used as nanocarriers for bovine-serum albumin and foot-and-mouth disease virus-like-particles.

Liu et al. [47] synthesized DMSNs with a particle size (156 ± 11 nm), an average pore size of 22 nm, a large surface area of 637 $m^2\ g^{-1}$, and a high pore volume of 3.08 $cm^3\ g^{-1}$ for delivering foot-and-mouth disease virus-like particles (FMD VLPs) protein and bovine serum albumin (BSA). The results showed that the synthesized DMSNs exhibited excellent protein loading capacity, good biocompatibility and hemocompatibility, and efficient cellular uptake. The immunization and adjuvant effect on guinea pigs showed that the synthesized DMSNs induced humoral immune response and protection against FMDV infection.

Certain studies exploring the effect of the spiky and rough surface of DMSNs found that the surface topology of DMSNs is a critical feature that improved the loading of smaller NPs within the principal structure [278]. In one such study, DMSNs were synthesized to evaluate their antibacterial properties. *In vitro* results revealed that the DMSNs caused effective inhibition of *E. coli* and *S. aureus* survival. These results are crucial as they pave the way for the design of efficient antibacterial agents. Beitzinger et al. isolated a microbial peptide named NapFab from bronchoalveolar lavage and optimized it to improve solubility in an aqueous solution and increase the positive charge to support the interaction with the negatively charged mycobacterial cell wall. The peptide was loaded into a DMSN carrier and administered to *Mycobacterium tuberculosis (Mtb) in vitro*. The antimycobacterial property of NapFab was significantly enhanced when encapsulated compared to free NapFab. Moreover, *Mtb*-infected macrophages incubated with NapFab-DMSNs showed an accumulation of DMSNs in the early and late endosomes, showing the effective peptide transport in the cells and thereby efficiently killing *Mtb* [279].

For inflammation, DMSNs have successfully been used to co-deliver ibuprofen (IBU) and BSA (as a protein model) using DMSNs modified with amino groups in the inner pores [23]. In the case of psoriasis, an inflammatory skin disorder, Mo et al. used Erianin-loaded DMSNs to reduce keratinocyte proliferation. Erianin is a potent inhibitor of keratinocyte proliferation and is also known to suppress tumor growth angiogenesis [280]. In this study, Erianin-loaded DMSNs showed a stronger anti-proliferative and pro-apoptotic effect than free Erianin in HaCaT cells. Moreover, when DMSNs were embedded in a hydrogel, the drug retention in porcine skin was better than only Erianin-loaded hydrogels. Moreover, the DMSNs showed pore-size-dependent anti-proliferative and anti-apoptotic effects against cells via the mitochondrial signaling pathway. Such DMSN systems can be used for the treatment of keratinocyte-related diseases [281]. Besides, DMSNs have shown effectiveness in arthritis therapy. *In vivo* administration of S-propargyl-cysteine (SPRC)-loaded DMSNs suppressed LPS-induced pro-inflammatory cytokines in a rat model of autoimmune arthritis. The DMSNs were designed to increase the expression of cystathionine ɣ-lyase, an enzyme that produces H_2S. The administration of the particles exerted anti-inflammatory properties. The $t_{1/2}$ of SRPC improved drastically to 17.1 h, compared to only 1.6 h for the free-SPRC group. Moreover, DMSNs did not induce any tissue damage and had a low toxicity. With a pore size of 10 nm, DMSNs were shown to be favorable and biocompatible for countering inflammation in arthritic rats [282]. Besides, DMSNs can be utilized as carriers of unstable products like antioxidants. For instance, due to the pronounced properties of 5-HM (5-hydroxymethylfurfural) on skin treatments, it has gained great attention in skin disorder therapies and cosmetic products. 5-HM can directly be applied to the skin, however, rapidly loses its bioactivity. The tunable characteristics of DMSNs, make these nanocarriers a good candidate for directly delivering the 5-HM to the skin [100].

Macrophages can be divided into several subtypes; they contribute to inflammation, tissue damage, regenerative medicine, and tissue remodeling [283]. The M1 type (“classically activated”)

macrophages are related to inflammation and tissue damage. In contrast, the M2 type ("alternatively activated") macrophages are involved in tissue remodeling and regeneration [227]. The switching of M1 to M2 macrophages has an undeniable role in restoring tissue homeostasis after injury or infection [284]. Recently, it has been shown that diabetes could be worsened by M1 but amended by M2 macrophages [285]. IL-4 is an anti-inflammatory cytokine with type-switching of M1 to M2 macrophage capability, so local delivery of this cytokine can be a suitable choice in dealing with diabetes. DMSNs were used to load IL-4. These NPs did not induce inflammatory responses, which is vital for the polarization of anti-inflammatory M2 macrophages.

5.5. Theranostics

Theranostic is a term used to integrate imaging and therapeutic technologies simultaneously [286]. The use of NPs-based contrast agents has numerous advantages over conventional contrast agents, including the ability to bind ligands for targeting diseased sites, signals amplification due to high loading, reducing the toxicity of some contrast agents, follow up the treatment efficacy, and use them as theranostic agents. Some NPs used as contrast agents and can convert one type of energy into another one. For example, gold NPs can transform near-infrared irradiation into heat. Subsequently, these heat propagated vibrations can be detected by ultrasound equipment as a photoacoustic imaging system [287]. The main advantage of the theranostic system is that it enables monitoring therapeutic efficacy by following the diseased site even for several hours to several days after treatment. As previously mentioned, the high surface area of the DMSNs gives them unique characteristics to act as carriers and use in various applications. For example, DMSNs were chosen to load radio-dense metals like gold (Au) and tantalum oxide (TaOx). The gold and tantalum oxide-loaded DMSNs were then administered for imaging and treating ovarian cancer. In the result obtained by Kashfi-Sadabad et al. [103], Au and TaOx DMSNs were injected intraperitoneally in a mouse model of ovarian cancer. Au and TaOx DMSNs accumulated and penetrated the cancerous organ and acted as an improved contrast agent resulting in higher-quality CT scan images.

Combining DMSNs with a relatively new non-invasive strategy like PDT can enhance the anti-tumor activity of therapeutic agents. Nevertheless, the efficiency of PDT is limited by the hypoxia medium of TME. Researchers have recently developed a multifunctional nano theranostic system based on DMSNs containing up-conversion NP (UCNPs) to create trimodal (UCL/MRI/CT) bioimaging and synergistic CDT/PDT/gas strategy for cancer therapy. These NP were composed of copper peroxide nanodots, chlorin e6 (Ce6), and polyethylene glycol (PEG) (UCNPs@dMSN-SNO@CuO2−Ce6-PEG) [108]. After endocytosis of the nanocomposites mentioned above, nanodots are fragmented in the acidic environment of TME, permitting the propagation of copper ions in the cells and subsequent production of H_2O_2 to achieve an efficient therapy [108].

6. Safety and toxicity

As discussed above, DMSNs are promising nanoplatforms for developing both imaging and therapeutic systems. However, safety and toxicity issues are still a concern in the biomedical application of nanoparticles. Several studies confirmed the biocompatibility of silica NPs, their possible toxicity and severity controlled by several factors in which the dose and administration exposure play a crucial role. The cytotoxicity of nanomaterials can be divided into two categories: 1) Toxicity due to the remnant solvents, surfactants, and chemicals used in the manufacturing of NPs. 2) Toxicity is associated with physicochemical properties, such as high zeta potential, shape, and size. For example, zeta potentials higher than 30 mV can damage cell membranes. Also, small NPs (less than 5 nm) can lead to genotoxicity in cells by disrupting various biological structures such as focal adhesion proteins (FAP) or interacting with transcription factors that cause tumorigenesis mutations. In addition to these two main toxic mechanisms, other routes have been discovered regarding the toxicity caused by NPs. For instance, an important issue is the leaking of toxic ions or molecules that formed the NP after degradation in endo/lysosomal compartments. This cytotoxicity strongly depends on the composition of NP.

The common examination for evaluation of nano-based materials biocompatibility is a hemolysis test [288]. According to the ISO/TR7405 standard, the maximum acceptable rate of hemolysis risk for any formulation should be under 5% [227]. In the case of DMSNs, it was demonstrated that manipulating the structure with certain compounds can increase their biocompatibility. For instance, Ca@DMSNs-FA displayed better hemocompatibility than pristine DMSNs at high concentrations due to the binding of the silanol group (Si−OH) of DMSNs with the phosphatidylcholine-rich RBC membrane [227]. For instance, stellated fibrous silica nanospheres (a type of DMSNs) did not show clear acute toxicity *in vivo* even up to seven days after administration [289].

Another safety issue is related to the possible accumulation of nanoparticles in the body. As a result, when designing NPs, one must carefully consider their application and excretion method. The excretion of NPs from the body occurred in two ways. NPs with a molecular weight (MW) less than 5.5 kDa or 10 nm in size are filtered from the kidneys. NPs above these amounts are mainly removed from the hepatobiliary pathway [reference]. In this case, NPs are collected by the RES system and delivered to hepatocyte cells, and finally excreted in the feces through conjugation with bilirubin. This pathway is slower compared to renal clearance. In the case of mesoporous silica materials, recent studies have demonstrated the biodegradability of these materials and their excretion through the renal pathway. It is well established that mesoporous silica metabolizes to orthosilicic acid (Si(OH)4), which is well-tolerated by the body and finally eliminated by urine [73]. Besides, some studies showed that silica-based nanoparticles could also be excreted in a lower proportion by the hepatobiliary route. One critical factor that profoundly affects silica-based nanoparticles' safety and thus clearance is their porous structure. The biphasic stratification approach in the synthesis of DMNS causes better degradability which is another crucial factor in the safety of DMNSs [31]. Besides, the morphology of nanoparticles can also be a key factor to improve their biocompatibility. For instance, the head-tail asymmetrical structure of silica NPs shows higher hemocompatibility compared to symmetrical ones [222]. The physicochemical properties of the nanoparticles are critical factors to achieve biocompatibility. They determine their pharmacokinetics and biodistribution profile in the body, which finally determines the clearance process. More research efforts are still needed to elucidate the biocompatibility and clearance of the nanoparticles to bring these promising delivery systems from bench to bedside.

7. Conclusions and future directions

The large pore size of DMSNs makes them an excellent candidate for theranostics due to their central-radial pore channels and highly accessible internal surface. These features enable the utilization of DMSNs as a next-generation multifunctional nanocarrier with a wide range of payloads and diverse functionalities. Moreover, DMSNs have better biodegradability and safety profiles compared to other silica nanoparticles due to the dendritic

morphology that facilitates biodegradation. The above properties extend the usability of DMSNs to antimicrobial therapies, vaccine development, tissue engineering, and immunotherapeutics. We elucidated the recent progress made on biomedical applications of DMSNs in various areas with a focus on anti-tumor therapies along with a comprehensive review of the synthesis strategies and characterization. With increasing interest in DMSN synthesis and application, this review serves as an essential tool and a short guide to enable future researchers to optimize the synthesis mechanism of DMSNs and design novel therapies for life-threatening conditions. Despite the advances in the development of DMSNs, the research on their application is still in an early stage and much more research is expected in a near future.

Future research needs to be focused on exploiting the potential of these DMSNs in different biomedical applications. Besides, the structure of DMSNs facilitates the development of mesoporous silica materials with faster degradation rates. Although the FDA recognizes silica, and its related degradation products, as “generally recognized as safe” (GRAS), a slower degradability in the body could lead to bioaccumulation and thus long-term toxicity resulting in diseases. Thus, the development of more easily clearable nanoparticles as DMSNs would be beneficial for achieving a clinical translation. Nevertheless, many efforts are still needed, and more studies evaluating the safety and fate of these materials at a preclinical level are required. Even though some challenges have still to be overcome, all the findings highlighted in this review suggested the suitability of DMSNs for further advanced applications in biomedicine. The benefit-to-risk ratio must be evaluated for each newly designed nanomaterial as well as consider the final biomedical application. Several new advances in the field of DMSNs can be expected in the near future, and we hope this review has given insights into the rational design of DMSNs nanoparticles and their future application.

Declaration of competing interest

The authors declare that they have no known competing financial interests or personal relationships that could have appeared to influence the work reported in this paper.

Data availability

Data will be made available on request.

Acknowledgments

T. K. acknowledges the support from the National Health and Medical Research Council of Australia (NHMRC) for the Early Career Fellowship (GNT1143296) and the University of New South Wales for support and the Scientia Grant. T.K. and G. R. K. also thank Australian Research Council (ARC) for the Discovery project grant (DP200102723). Some of the figures for the graphical abstract were adopted from smart.servier.com. R.M.-M. and A.G.-F. acknowledge the financial support from Project PROMETEO 2018/024 from the Generalitat Valenciana and Project RTI2018-100910-B-C41 funded by MCIN/AEI/10.13039/501100011033/and FEDER A way to make Europe.

References

[1] I. Khan, K. Saeed, I. Khan, Arab. J. Chem. 12 (2019) 908–931.
[2] B. Yu, H.C. Tai, W. Xue, L.J. Lee, R.J. Lee, Mol. Membr. Biol. 27 (2010) 286–298.
[3] M. Bhia, M. Motallebi, B. Abadi, A. Zarepour, M. Pereira-Silva, F. Saremnejad, A.C. Santos, A. Zarrabi, A. Melero, S.M. Jafari, M. Shakibaei, Pharmaceutics 13 (2021).
[4] K.F. Pirollo, E.H. Chang, Trends Biotechnol. 26 (2008) 552–558.
[5] L. Nobs, F. Buchegger, R. Gurny, E. Allémann, J. Pharmaceut. Sci. 93 (2004) 1980–1992.
[6] H. Sahrayi, E. Hosseini, S. Karimifard, N. Khayam, S.M. Meybodi, S. Amiri, M. Bourbour, B. Farasati Far, I. Akbarzadeh, M. Bhia, C. Hoskins, C. Chaiyasut, Pharmaceuticals 15 (2022).
[7] M.M. Attwood, J. Jonsson, M. Rask-Andersen, H.B. Schiöth, Nat. Rev. Drug Discov. 19 (2020) 695–710.
[8] Y.-J. Yu, J.-L. Xing, J.-L. Pang, S.-H. Jiang, K.-F. Lam, T.-Q. Yang, Q.-S. Xue, K. Zhang, P. Wu, ACS Appl. Mater. Interfaces 6 (2014) 22655–22665.
[9] E. Abbasi, S.F. Aval, A. Akbarzadeh, M. Milani, H.T. Nasrabadi, S.W. Joo, Y. Hanifehpour, K. Nejati-Koshki, R. Pashaei-Asl, Nanoscale Res. Lett. 9 (2014) 247.
[10] D.H. Everett, Pure Appl. Chem. 31 (1972) 577–638.
[11] H. Lv, Y. Xing, Y. Wang, X. Li, X. Zhang, X. Du, J. Alloys Compd. 815 (2020), 152641.
[12] J.S. Beck, J.C. Vartuli, W.J. Roth, M.E. Leonowicz, C.T. Kresge, K.D. Schmitt, C.T.W. Chu, D.H. Olson, E.W. Sheppard, S.B. McCullen, J.B. Higgins, J.L. Schlenker, J. Am. Chem. Soc. 114 (1992) 10834–10843.
[13] H. Lin, K. Cui, Y. Yao, Q. Cai, Q. Feng, H. Li, Chem. Lett. 34 (2005) 918–919.
[14] Q. Cai, Y. Geng, X. Zhao, K. Cui, Q. Sun, X. Chen, Q. Feng, H. Li, E.G. Vrieling, Microporous Mesoporous Mater. 108 (2008) 123–135.
[15] Y. Xu, Y. Zhu, X. Li, H. Morita, N. Hanagata, Mater. Express 6 (2016) 116–126.
[16] M. Kalantari, T. Ghosh, Y. Liu, J. Zhang, J. Zou, C. Lei, C. Yu, ACS Appl. Mater. Interfaces 11 (2019) 13264–13272.
[17] Z. Li, L. Rong, ACS Appl. Mater. Interfaces 13 (2021) 23469–23480.
[18] Z. Li, L. Rong, Biomater. Sci. 8 (2020) 6272–6285.
[19] Z. Liu, J. Ru, S. Sun, Z. Teng, H. Dong, P. Song, Y. Yang, H. Guo, J. Mater. Chem. B 7 (2019) 3446–3454.
[20] X. Huang, Z. Tao, J.C. Praskavich, A. Goswami, J.F. Al-Sharab, T. Minko, V. Polshettiwar, T. Asefa, Langmuir 30 (2014) 10886–10898.
[21] D. Shen, L. Chen, J. Yang, R. Zhang, Y. Wei, X. Li, W. Li, Z. Sun, H. Zhu, A.M. Abdullah, A. Al-Enizi, A.A. Elzatahry, F. Zhang, D. Zhao, ACS Appl. Mater. Interfaces 7 (2015) 17450–17459.
[22] C. Lei, C. Xu, A. Nouwens, C. Yu, J. Mater. Chem. B 4 (2016) 4975–4979.
[23] Y. Liu, B. Huang, J. Zhu, K. Feng, Y. Yuan, C. Liu, RSC Adv. 8 (2018) 40598–40610.
[24] Y. Wang, B. Zhang, X. Ding, X. Du, Nano Today 39 (2021), 101231.
[25] Y. Wang, X. Du, Z. Liu, S. Shi, H. Lv, J. Mater. Chem. 7 (2019) 5111–5152.
[26] P. Hao, B. Peng, B.-Q. Shan, T.-Q. Yang, K. Zhang, Nanoscale Adv. 2 (2020) 1792–1810.
[27] K. Thananukul, C. Kaewsaneha, P. Opaprakasit, N. Lebaz, A. Errachid, A. Elaissari, Adv. Drug Deliv. Rev. 174 (2021) 425–446.
[28] X. Du, S.Z. Qiao, Small 11 (2015) 392–413.
[29] D. Zhao, J. Feng, Q. Huo, N. Melosh, G.H. Fredrickson, B.F. Chmelka, G.D. Stucky, Science 279 (1998) 548.
[30] A. Schwanke, R. Balzer, S. Pergher, Microporous and Mesoporous Materials from Natural and Inexpensive Sources, 2017.
[31] D. Shen, J. Yang, X. Li, L. Zhou, R. Zhang, W. Li, L. Chen, R. Wang, F. Zhang, D. Zhao, Nano Lett. 14 (2014) 923–932.
[32] M. Wu, Q. Meng, Y. Chen, Y. Du, L. Zhang, Y. Li, L. Zhang, J. Shi, Adv. Mater. 27 (2015) 215–222.
[33] P.-C. Liu, Y.-J. Yu, B. Peng, S.-Y. Ma, T.-Y. Ning, B.-Q. Shan, T.-Q. Yang, Q.-S. Xue, K. Zhang, P. Wu, Green Chem. 19 (2017) 5575–5581.
[34] R. Narayan, U.Y. Nayak, A.M. Raichur, S. Garg, Pharmaceutics 10 (2018) 118.
[35] Y. Dai, D. Yang, D. Yu, S. Xie, B. Wang, J. Bu, B. Shen, W. Feng, F. Li, Nanoscale 12 (2020) 5075–5083.
[36] M.-R. Wu, B. Jusiak, T.K. Lu, Nat. Rev. Cancer 19 (2019) 187–195.
[37] X. Zhang, X.-F. Sun, B. Shen, H. Zhang, Cancers 11 (2019) 172.
[38] A. Kakkar, G. Traverso, O.C. Farokhzad, R. Weissleder, R. Langer, Nat. Rev. Chem 1 (2017), 0063.
[39] P. Sharma, H.A. Cho, J.-W. Lee, W.S. Ham, B.C. Park, N.-H. Cho, Y.K. Kim, Nanoscale 9 (2017) 15371–15378.
[40] J. Zhang, J. Liu, S. Lu, H. Zhu, D. Aili, R. De Marco, Y. Xiang, M. Forsyth, Q. Li, S.P. Jiang, ACS Appl. Mater. Interfaces 9 (2017) 31922–31930.
[41] Y. Zhou, G. Quan, Q. Wu, X. Zhang, B. Niu, B. Wu, Y. Huang, X. Pan, C. Wu, Acta Pharm. Sin. B 8 (2018) 165–177.
[42] C. Lei, P. Liu, B. Chen, Y. Mao, H. Engelmann, Y. Shin, J. Jaffar, I. Hellstrom, J. Liu, K.E. Hellstrom, J. Am. Chem. Soc. 132 (2010) 6906–6907.
[43] J.N. Talbert, L.-S. Wang, B. Duncan, Y. Jeong, S.M. Andler, V.M. Rotello, J.M. Goddard, Biomacromolecules 15 (2014) 3915–3922.
[44] J. Gao, Y. Wang, Y. Du, L. Zhou, Y. He, L. Ma, L. Yin, W. Kong, Y. Jiang, Chem. Eng. J. 317 (2017) 175–186.
[45] Y. Song, Y. Ding, F. Wang, Y. Chen, Y. Jiang, Chem. Eng. J. 375 (2019), 121968.
[46] K.M. Fuentes, L.L. Coria-Oriundo, S. Wirth, S.A. Bilmes, J. Porous Mater. 28 (2021) 261–269.
[47] G. Bai, X. Xu, Q. Dai, Q. Zheng, Y. Yao, S. Liu, C. Yao, Analyst 144 (2019) 481–487.
[48] V. Califano, F. Sannino, A. Costantini, J. Avossa, S. Cimino, A. Aronne, J. Phys. Chem. C 122 (2018) 8373–8379.
[49] Y. Yong, Y.-X. Bai, Y.-F. Li, L. Lin, Y.-J. Cui, C.-G. Xia, Process Biochem. 43 (2008) 1179–1185.
[50] D. Tarn, C.E. Ashley, M. Xue, E.C. Carnes, J.I. Zink, C.J. Brinker, Acc. Chem. Res. 46 (2013) 792–801.
[51] E. Juère, R. Caillard, D. Marko, G. Del Favero, F. Kleitz, Chem. Eur. J. 26 (2020) 5195–5199.

[52] H.-K. Han, G.L. Amidon, AAPS PharmSci 2 (2000) 48–58.
[53] A. Kienzle, S. Kurch, J. Schlöder, C. Berges, R. Ose, J. Schupp, A. Tuettenberg, H. Weiss, J. Schultze, S. Winzen, M. Schinnerer, K. Koynov, M. Mezger, N.K. Haass, W. Tremel, H. Jonuleit, Adv. Healthc. Mater. 6 (2017).
[54] D. Hanahan, R.A. Weinberg, Cell 144 (2011) 646–674.
[55] M. Bhia, H.F. Rajani, N. Mohammadkhani, S.M. Jafari, Saffron (Crocins) against cancer, in: S.M. Jafari, S.M. Nabavi, A.S. Silva (Eds.), Nutraceuticals and Cancer Signaling: Clinical Aspects and Mode of Action, Springer International Publishing, Cham, 2021, pp. 323–365.
[56] M. Kong, J. Tang, Q. Qiao, T. Wu, Y. Qi, S. Tan, X. Gao, Z. Zhang, Theranostics 7 (2017) 3276.
[57] P.L. Abbaraju, Y. Yang, M. Yu, J. Fu, C. Xu, C. Yu, Chem. Asian J. 12 (2017) 1465–1469.
[58] L. Schwartz, C. T Supuran, K. O Alfarouk, Anti-cancer agents in medicinal chemistry (Formerly Current Medicinal Chemistry-Anti-Cancer Agents), 17, 2017, pp. 164–170.
[59] C. Alvarez-Lorenzo, V.Y. Grinberg, T.V. Burova, A. Concheiro, Int. J. Pharm. 579 (2020), 119157.
[60] V.P. Torchilin, Nat. Rev. Drug Discov. 13 (2014) 813–827.
[61] C. He, X. Zhuang, Z. Tang, H. Tian, X. Chen, Adv. Healthc. Mater. 1 (2012) 48–78.
[62] E. Aznar, M. Oroval, L. Pascual, J.R. Murguía, R. Martínez-Máñez, F. Sancenón, Chem. Rev. 116 (2016) 561–718.
[63] A. García-Fernández, E. Aznar, R. Martínez-Máñez, F. Sancenón, Small 16 (2020), 1902242.
[64] A. Raza, T. Rasheed, F. Nabeel, U. Hayat, M. Bilal, H. Iqbal, Molecules 24 (2019) 1117.
[65] H. Hatakeyama, Chem. Pharm. Bull. 65 (2017) 612–617.
[66] S. Malekmohammadi, H. Hadadzadeh, Z. Amirghofran, J. Mol. Liq. 265 (2018) 797–806.
[67] S.J. Hewlings, D.S. Kalman, Foods 6 (2017) 92.
[68] H. Fan, B. Li, Z. Shi, L. Zhao, K. Wang, D. Qiu, Ceram. Int. 44 (2018) 2345–2350.
[69] M. Huang, L. Liu, S. Wang, H. Zhu, D. Wu, Z. Yu, S. Zhou, Langmuir 33 (2017) 519–526.
[70] J. Wang, Y. Wang, Q. Liu, L. Yang, R. Zhu, C. Yu, S. Wang, ACS Appl. Mater. Interfaces 8 (2016) 26511–26523.
[71] Y. Lu, Y. Yang, Z. Gu, J. Zhang, H. Song, G. Xiang, C. Yu, Biomaterials 175 (2018) 82–92.
[72] X. Du, F. Kleitz, X. Li, H. Huang, X. Zhang, S.-Z. Qiao, Adv. Funct. Mater. 28 (2018), 1707325.
[73] Y. Fei, M. Li, Y. Li, X. Wang, C. Xue, Z. Wu, J. Xu, Z. Xiazeng, K.-Y. Cai, Z. Luo, Nanoscale 12 (2020) 16102–16112.
[74] X. Du, B. Shi, Y. Tang, S. Dai, S.Z. Qiao, Biomaterials 35 (2014) 5580–5590.
[75] T.M. Guardado-Alvarez, L.S. Devi, J.-M. Vabre, T.A. Pecorelli, B.J. Schwartz, J.-O. Durand, O. Mongin, M. Blanchard-Desce, J.I. Zink, Nanoscale 6 (2014) 4652–4658.
[76] K. Gwon, E.-J. Jo, A. Sahu, J.Y. Lee, M.-G. Kim, G. Tae, Mater. Sci. Eng. C 90 (2018) 77–84.
[77] A. Schroeder, R. Honen, K. Turjeman, A. Gabizon, J. Kost, Y. Barenholz, J. Contr. Release 137 (2009) 63–68.
[78] S. Mura, J. Nicolas, P. Couvreur, Nat. Mater. 12 (2013) 991–1003.
[79] J. Ge, E. Neofytou, T.J. Cahill III, R.E. Beygui, R.N. Zare, ACS Nano 6 (2012) 227–233.
[80] M. Moros, J. Idiago-López, L. Asín, E. Moreno-Antolín, L. Beola, V. Grazú, R.M. Fratila, L. Gutiérrez, J.M. de la Fuente, Adv. Drug Deliv. Rev. 138 (2019) 326–343.
[81] J.F. Liu, B. Jang, D. Issadore, A. Tsourkas, Wiley Interdisciplinary Reviews: Wiley Interdiscip. Rev. Comput. Mol. Sci. 11 (2019), e1571.
[82] T.E. Torres, E. Lima, M.P. Calatayud, B. Sanz, A. Ibarra, R. Fernández-Pacheco, A. Mayoral, C. Marquina, M.R. Ibarra, G.F. Goya, Sci. Rep. 9 (2019) 1–11.
[83] M.A. Ward, T.K. Georgiou, Polymers 3 (2011) 1215–1242.
[84] V. Pillay, T.S. Tsai, Y.E. Choonara, L.C. du Toit, P. Kumar, G. Modi, D. Naidoo, L.K. Tomar, C. Tyagi, V.M. Ndesendo, J. Biomed. Mater. Res. 102 (2014) 2039–2054.
[85] C. Schneider, R. Langer, D. Loveday, D. Hair, J. Contr. Release 262 (2017) 284–295.
[86] S. Malekmohammadi, H. Hadadzadeh, S. Rezakhani, Z. Amirghofran, ACS Biomater. Sci. Eng. 5 (2019) 4405–4415.
[87] S. Hajebi, N. Rabiee, M. Bagherzadeh, S. Ahmadi, M. Rabiee, H. Roghani-Mamaqani, M. Tahriri, L. Tayebi, M.R. Hamblin, Acta Biomater. 92 (2019) 1–18.
[88] L. Li, W.-W. Yang, D.-G. Xu, J. Drug Target. 27 (2019) 423–433.
[89] D. Liu, F. Yang, F. Xiong, N. Gu, Theranostics 6 (2016) 1306.
[90] Z. Zhao, A. Ukidve, J. Kim, S. Mitragotri, Cell 181 (2020) 151–167.
[91] M. Manzano, M. Vallet-Regí, Adv. Funct. Mater. 30 (2020), 1902634.
[92] C. Mathes, A. Melero, P. Conrad, T. Vogt, L. Rigo, D. Selzer, W.A. Prado, C. De Rossi, T.M. Garrigues, S. Hansen, S.S. Guterres, A.R. Pohlmann, R.C.R. Beck, C.M. Lehr, U.F. Schaefer, J. Contr. Release 223 (2016) 207–214.
[93] A. Castoldi, C. Herr, J. Niederstraßer, H.I. Labouta, A. Melero, S. Gordon, N. Schneider-Daum, R. Bals, C.-M. Lehr, Eur. J. Pharm. Biopharm. 118 (2017) 62–67.
[94] A.J. Guillot, E. Jornet-Mollá, N. Landsberg, C. Milián-Guimerá, M.C. Montesinos, T.M. Garrigues, A. Melero, Pharmaceutics 13 (2021).
[95] M.M. Abeer, P. Rewatkar, Z. Qu, M. Talekar, F. Kleitz, R. Schmid, M. Lindén, T. Kumeria, A. Popat, J. Contr. Release 326 (2020) 544–555.
[96] F. Nowroozi, S. Dadashzadeh, H. Soleimanjahi, A. Haeri, S. Shahhosseini, J. Javidi, H. Karimi, Nanomedicine 13 (2018) 2201–2219.
[97] D. Babadi, S. Dadashzadeh, M. Osouli, Z. Abbasian, M.S. Daryabari, S. Sadrai, A. Haeri, J. Drug Deliv. Sci. Technol. 62 (2021), 102324.
[98] S. Alavi, A. Haeri, I. Mahlooji, S. Dadashzadeh, Pharmaceut. Res. 37 (2020) 119.
[99] M. Zahiri, M. Babaei, K. Abnous, S.M. Taghdisi, M. Ramezani, M. Alibolandi, J. Cell. Physiol. 235 (2020) 1036–1050.
[100] X. Niu, Z. Wang, L. Zhang, Y. Quan, K. Wei, RSC Adv. 8 (2018) 25021–25030.
[101] E. Juère, G. Del Favero, F. Masse, D. Marko, A. Popat, J. Florek, R. Caillard, F. Kleitz, Eur. J. Pharm. Biopharm. 151 (2020) 171–180.
[102] M.M. Abeer, A.K. Meka, N. Pujara, T. Kumeria, E. Strounina, R. Nunes, A. Costa, B. Sarmento, S.Z. Hasnain, B.P. Ross, A. Popat, Pharmaceutics 11 (2019).
[103] R. Kashfi-Sadabad, L. Gonzalez-Fajardo, D. Hargrove, B. Ahmadi, D. Munteanu, S. Shahbazmohamadi, M. Jay, X. Lu, Part. Part. Syst. Char. 36 (2019), 1900058.
[104] C. Deng, Y. Liu, F. Zhou, M. Wu, Q. Zhang, D. Yi, W. Yuan, Y. Wang, J. Colloid Interface Sci. 593 (2021) 424–433.
[105] J. Ma, H. Sun, Y. Zhang, D. Chen, H. Hu, J. Drug Deliv. Sci. Technol. 62 (2021), 102387.
[106] B. Liu, Z. Wang, T. Li, Q. Sun, S. Dong, C. Zhong, D. Yang, F. He, S. Gai, P. Yang, ACS Appl. Mater. Interfaces 12 (2020) 45772–45788.
[107] T. Li, F. He, B. Liu, T. Jia, B. Shao, R. Zhao, H. Zhu, D. Yang, S. Gai, P. Yang, ACS Appl. Mater. Interfaces 12 (2020).
[108] S. Liu, W. Li, S. Dong, F. Zhang, Y. Dong, B. Tian, F. He, S. Gai, P. Yang, Nanoscale 12 (2020).
[109] K. Ulbrich, K. Hola, V. Subr, A. Bakandritsos, J. Tucek, R. Zboril, Chem. Rev. 116 (2016) 5338–5431.
[110] M.F. Attia, N. Anton, J. Wallyn, Z. Omran, T.F. Vandamme, J. Pharm. Pharmacol. 71 (2019) 1185–1198.
[111] J. Fang, H. Nakamura, H. Maeda, Adv. Drug Deliv. Rev. 63 (2011) 136–151.
[112] H. Maeda, Adv. Enzym. Regul. 41 (2001) 189–207.
[113] W. Arap, R. Pasqualini, E. Ruoslahti, Science 279 (1998) 377–380.
[114] S. Sindhwani, A.M. Syed, J. Ngai, B.R. Kingston, L. Maiorino, J. Rothschild, P. MacMillan, Y. Zhang, N.U. Rajesh, T. Hoang, Nat. Mater. 19 (2020) 566–575.
[115] L. Liu, T.K. Hitchens, Q. Ye, Y. Wu, B. Barbe, D.E. Prior, W.F. Li, F.-C. Yeh, L.M. Foley, D.J. Bain, Biochim. Biophys. Acta Gen. Subj. 1830 (2013) 3447–3453.
[116] G. Prencipe, S.M. Tabakman, K. Welsher, Z. Liu, A.P. Goodwin, L. Zhang, J. Henry, H. Dai, J. Am. Chem. Soc. 131 (2009) 4783–4787.
[117] T. Liu, H. Choi, R. Zhou, I.-W. Chen, Nano Today 10 (2015) 11–21.
[118] J.-W. Yoo, E. Chambers, S. Mitragotri, Curr. Pharmaceut. Des. 16 (2010) 2298–2307.
[119] Z. Amoozgar, Y. Yeo, Wiley Interdisciplinary Reviews: Wiley Interdiscip. Rev. Comput. Mol. Sci. 4 (2012) 219–233.
[120] J. Kopeček, P. Kopečková, Adv. Drug Deliv. Rev. 62 (2010) 122–149.
[121] D. Pozzi, V. Colapicchioni, G. Caracciolo, S. Piovesana, A.L. Capriotti, S. Palchetti, S. De Grossi, A. Riccioli, H. Amenitsch, A. Laganà, Nanoscale 6 (2014) 2782–2792.
[122] K.R. Chaudhari, M. Ukawala, A.S. Manjappa, A. Kumar, P.K. Mundada, A.K. Mishra, R. Mathur, J. Mönkkönen, R.S.R. Murthy, Pharmaceut. Res. 29 (2012) 53–68.
[123] C. Yagüe, M. Moros, V. Grazú, M. Arruebo, J. Santamaria, Chem. Eng. J. 137 (2008) 45–53.
[124] B. Thierry, L. Zimmer, S. McNiven, K. Finnie, C. Barbé, H.J. Griesser, Langmuir 24 (2008) 8143–8150.
[125] Y. Wang, J.E.Q. Quinsaat, T. Ono, M. Maeki, M. Tokeshi, T. Isono, K. Tajima, T. Satoh, S.-i. Sato, Y. Miura, Nat. Commun. 11 (2020) 1–12.
[126] M.H. Jazayeri, H. Amani, A.A. Pourfatollah, H. Pazoki-Toroudi, B. Sedighimoghaddam, Sens. Bio-sensing Res. 9 (2016) 17–22.
[127] V. Selvarajan, S. Obuobi, P.L.R. Ee, Front. Chem. 8 (2020) 602.
[128] C. von Baeckmann, H. Kählig, M. Lindén, F. Kleitz, J. Colloid Interface Sci. 589 (2021) 453–461.
[129] M. Amin, W. Huang, A.L. Seynhaeve, T.L. Ten Hagen, Pharmaceutics 12 (2020) 1007.
[130] S. Dissanayake, W.A. Denny, S. Gamage, V. Sarojini, J. Contr. Release 250 (2017) 62–76.
[131] P.T. Wong, S.K. Choi, Chem. Rev. 115 (2015) 3388–3432.
[132] J.D. Byrne, T. Betancourt, L. Brannon-Peppas, Adv. Drug Deliv. Rev. 60 (2008) 1615–1626.
[133] R. Bazak, M. Houri, S. El Achy, S. Kamel, T. Refaat, J. Cancer Res. Clin. Oncol. 141 (2015) 769–784.
[134] J. Yoo, C. Park, G. Yi, D. Lee, H. Koo, Cancers 11 (2019) 640.
[135] A.K. Pearce, R.K. O'Reilly, Bioconjugate Chem. 30 (2019) 2300–2311.
[136] A. Alibakhshi, F.A. Kahaki, S. Ahangarzadeh, H. Yaghoobi, F. Yarian, R. Arezumand, J. Ranjbari, A. Mokhtarzadeh, M. de la Guardia, J. Contr. Release 268 (2017) 323–334.
[137] C. Galustian, C.G. Park, W. Chai, M. Kiso, S.A. Bruening, Y.S. Kang, R.M. Steinman, T. Feizi, Int. Immunol. 16 (2004) 853–866.
[138] S.A. Lamprecht, M. Lipkin, Nat. Rev. Cancer 3 (2003) 601–614.
[139] M. Westphal, C.L. Maire, K. Lamszus, CNS Drugs 31 (2017) 723–735.
[140] D.-Y. Oh, Y.-J. Bang, Nat. Rev. Clin. Oncol. 17 (2020) 33–48.

[141] H. Liu, D. Jia, F. Yuan, F. Wang, D. Wei, X. Tang, B. Tian, S. Zheng, R. Sun, J. Shi, Q. Fan, Int. J. Pharm. 617 (2022), 121609.
[142] A. Sheikh, N.A. Alhakamy, S. Md, P. Kesharwani, Front. Pharmacol. 12 (2021) 803304.
[143] L.M. Ellis, D.J. Hicklin, Clin. Cancer Res. 14 (2008) 6371–6375.
[144] T. Kuwai, T. Nakamura, T. Sasaki, Y. Kitadai, J.-S. Kim, R.R. Langley, D. Fan, X. Wang, K.-A. Do, S.-J. Kim, Clin. Exp. Metastasis 25 (2008) 477–489.
[145] Z. Tao, H. Yang, Q. Shi, Q. Fan, L. Wan, X. Lu, Theranostics 7 (2017) 2261.
[146] P. Singh, J.M. Alex, F. Bast, Med. Oncol. 31 (2014) 805.
[147] J. Yue, S. Liu, R. Wang, X. Hu, Z. Xie, Y. Huang, X. Jing, Mol. Pharm. 9 (2012) 1919–1931.
[148] S. Lütje, S. Heskamp, G.M. Franssen, C. Frielink, A. Kip, M. Hekman, G. Fracasso, M. Colombatti, K. Herrmann, O.C. Boerman, Theranostics 9 (2019) 2924.
[149] G.J. Kim, S. Nie, Mater. Today 8 (2005) 28–33.
[150] I. Pastan, R. Hassan, Cancer Res. 74 (2014) 2907–2912.
[151] V. Nguyen, J.M. Conyers, D. Zhu, D.M. Gibo, J.F. Dorsey, W. Debinski, A. Mintz, Transl. Oncol. 4 (2011) 390–400.
[152] R.V. Lumsden, J.C. Worrell, D. Boylan, S.M. Walsh, J. Cramton, I. Counihan, S. O'Beirne, M.F. Medina, J. Gauldie, A. Fabre, Am. J. Physiol. Lung Cell Mol. Physiol. 308 (2015) L710–L718.
[153] L. Xing, Y. Xu, K. Sun, H. Wang, F. Zhang, Z. Zhou, J. Zhang, F. Zhang, B. Caliskan, Z. Qiu, Sci. Rep. 8 (2018) 1–13.
[154] B.A. Gartrell, C.-k. Tsao, M.D. Galsky, Urologic Oncology: Seminars and Original Investigations, Elsevier, 2013, pp. 1403–1407.
[155] K. Staflin, C.L.Z. de Zafra, L.K. Schutt, V. Clark, F. Zhong, M. Hristopoulos, R. Clark, J. Li, M. Mathieu, X. Chen, JCI Insight (2020) 5.
[156] P. Engel, L.-J. Zhou, D.C. Ord, S. Sato, B. Koller, T.F. Tedder, Immunity 3 (1995) 39–50.
[157] L. Martínez-Jothar, S. Doulkeridou, R.M. Schiffelers, J.S. Torano, S. Oliveira, C.F. van Nostrum, W.E. Hennink, J. Contr. Release 282 (2018) 101–109.
[158] J.M. Morachis, E.A. Mahmoud, A. Almutairi, Pharmacol. Rev. 64 (2012) 505–519.
[159] L. Zhang, D. Hu, M. Salmain, B. Liedberg, S. Boujday, Talanta 204 (2019) 875–881.
[160] E.A. Leed, J.O. Sofo, C.G. Pantano, Phys. Rev. B 72 (2005), 155427.
[161] P.A. Ellison, F. Chen, S. Goel, T.E. Barnhart, R.J. Nickles, O.T. DeJesus, W. Cai, ACS Appl. Mater. Interfaces 9 (2017) 6772–6781.
[162] Y. Jiao, S. Shen, Y. Sun, X. Jiang, W. Yang, Part. Part. Syst. Char. 32 (2015) 222–233.
[163] X. Cai, Y. Luo, Y. Song, D. Liu, H. Yan, H. Li, D. Du, C. Zhu, Y. Lin, Nanoscale 10 (2018) 22937–22945.
[164] L. Dai, Q. Zhang, J. Li, X. Shen, C. Mu, K. Cai, ACS Appl. Mater. Interfaces 7 (2015) 7357–7372.
[165] J.A. Flood-Garibay, M.A. Méndez-Rojas, Colloids Surf. A Physicochem. Eng. Asp. 615 (2021), 126236.
[166] S. Liu, Y. Zheng, J. Hu, Z. Wu, H. Chen, New J. Chem. 44 (2020) 17382–17390.
[167] J.-F. Cao, W. Xu, Y.-Y. Zhang, Y. Shu, J.-H. Wang, Anal. Chim. Acta 1104 (2020) 78–86.
[168] X. Wang, H. Wang, J. Tang, S. Wang, D. Shi, H. Shen, ACS Appl. Mater. Interfaces 12 (2020) 37906–37913.
[169] H. Shan, Y. Si, J. Yu, B. Ding, Chem. Eng. J. 417 (2021), 129211.
[170] G. Jiahu, L. Yucun, M. Hui, C. Tao, L. Weimin, D. Jun, Z. Lunchao, S.M. Sadeghzadeh, Catal. Lett. 150 (2020) 2003–2012.
[171] E.B. Yahya, A.M. Alqadhi, Life Sciences, 2021, 119087.
[172] J.H. Myung, S.J. Park, A.Z. Wang, S. Hong, Adv. Drug Deliv. Rev. 125 (2018) 36–47.
[173] K. Bromma, A. Bannister, A. Kowalewski, L. Cicon, D.B. Chithrani, Cancer Nanotechnol. 11 (2020) 8.
[174] Y. Sun, W. Ma, Y. Yang, M. He, A. Li, L. Bai, B. Yu, Z. Yu, Asian J. Pharm. Sci. 14 (2019) 581–594.
[175] H. Yamada, C. Urata, Y. Aoyama, S. Osada, Y. Yamauchi, K. Kuroda, Chem. Mater. 24 (2012) 1462–1471.
[176] S.P. Gomes, M. Odložilíková, M.G. Almeida, A.N. Araújo, C.M. Couto, M.C.B. Montenegro, J. Pharmaceut. Biomed. Anal. 43 (2007) 1376–1381.
[177] I. San-Millán, G.A. Brooks, Carcinogenesis 38 (2017) 119–133.
[178] J. Tang, A.K. Meka, S. Theivendran, Y. Wang, Y. Yang, H. Song, J. Fu, W. Ban, Z. Gu, C. Lei, Angew. Chem. 132 (2020) 22238–22246.
[179] J. Tang, A.K. Meka, S. Theivendran, Y. Wang, Y. Yang, H. Song, J. Fu, W. Ban, Z. Gu, C. Lei, S. Li, C. Yu, Angew. Chem. Int. Ed. 59 (2020) 22054–22062.
[180] Y. Huang, K. Shen, Y. Si, C. Shan, H. Guo, M. Chen, L. Wu, J. Colloid Interface Sci. 583 (2021) 166–177.
[181] X. Zhang, J. Du, Z. Guo, J. Yu, Q. Gao, W. Yin, S. Zhu, Z. Gu, Y. Zhao, Adv. Sci. 6 (2019), 1801122.
[182] X. Zhang, G. Tian, W. Yin, L. Wang, X. Zheng, L. Yan, J. Li, H. Su, C. Chen, Z. Gu, Adv. Funct. Mater. 25 (2015) 3049–3056.
[183] H.-J. Xiang, L. An, W.-W. Tang, S.-P. Yang, J.-G. Liu, Chem. Commun. 51 (2015) 2555–2558.
[184] D.A. Riccio, M.H. Schoenfisch, Chem. Soc. Rev. 41 (2012) 3731–3741.
[185] H.-J. Xiang, Q. Deng, L. An, M. Guo, S.-P. Yang, J.-G. Liu, Chem. Commun. 52 (2016) 148–151.
[186] I. Munaweera, Y. Shi, B. Koneru, A. Patel, M.H. Dang, A.J. Di Pasqua, K.J. Balkus Jr., J. Inorg. Biochem. 153 (2015) 23–31.
[187] Z. Huang, Technol. Cancer Res. Treat. 4 (2005) 283–293.
[188] K.B. Reeds, T.D. Ridgway, R.G. Higbee, M.D. Lucroy, Vet. Comp. Oncol. 2 (2004) 157–163.
[189] J. Liu, X. Zhao, W. Nie, Y. Yang, C. Wu, W. Liu, K. Zhang, Z. Zhang, J. Shi, Theranostics 11 (2021) 379–396.
[190] L. Zou, H. Wang, B. He, L. Zeng, T. Tan, H. Cao, X. He, Z. Zhang, S. Guo, Y. Li, Theranostics 6 (2016) 762–772.
[191] P. Zhao, L. Qiu, S. Zhou, L. Li, Z. Qian, H. Zhang, Int. J. Nanomed. 16 (2021) 2107–2121.
[192] X.I.N.Y.G.U.O.Z.G.A.O.W.Z.H.U.Y.W.Y.R.A.N.R. Wu Liting, Y. Xiaoying, Chemical Research in Chinese Universities, 0.
[193] C. Li, X.-Q. Yang, J. An, K. Cheng, X.-L. Hou, X.-S. Zhang, X.-L. Song, K.-C. Huang, W. Chen, B. Liu, Y.-D. Zhao, T.-C. Liu, Theranostics 9 (2019) 7666–7679.
[194] S. Malekmohammadi, H. Hadadzadeh, H. Farrokhpour, Z. Amirghofran, Soft Matter 14 (2018) 2400–2410.
[195] K. Tachibana, L.B. Feril Jr., Y. Ikeda-Dantsuji, Ultrasonics 48 (2008) 253–259.
[196] X. Pan, H. Wang, S. Wang, X. Sun, L. Wang, W. Wang, H. Shen, H. Liu, Sci. China Life Sci. 61 (2018) 415–426.
[197] J. Zuo, M. Huo, L. Wang, J. Li, Y. Chen, P. Xiong, J. Mater. Chem. B 8 (2020) 9084–9093.
[198] Z. Tang, Y. Liu, M. He, W. Bu, Angew. Chem. Int. Ed. 58 (2019) 946–956.
[199] M. Huo, L. Wang, Y. Chen, J. Shi, Nat. Commun. 8 (2017) 357.
[200] P. Wang, C. Liang, J. Zhu, N. Yang, A. Jiao, W. Wang, X. Song, X. Dong, ACS Appl. Mater. Interfaces 11 (2019) 41140–41147.
[201] Y. Dong, S. Dong, Z. Wang, L. Feng, Q. Sun, G. Chen, F. He, S. Liu, W. Li, P. Yang, ACS Appl. Mater. Interfaces 12 (2020) 52479–52491.
[202] Y. Xing, Q. Pan, X. Du, T. Xu, Y. He, X. Zhang, ACS Appl. Mater. Interfaces 11 (2019) 10426–10433.
[203] B. Shi, X. Du, J. Chen, L. Fu, M. Morsch, A. Lee, Y. Liu, N. Cole, R. Chung, Small 13 (2017), 1603966.
[204] A. Salvador, M. Igartua, R.M. Hernández, J.L. Pedraz, J. Drug Deliv. (2011) 2011.
[205] B.S. Zolnik, Á. González-Fernández, N. Sadrieh, M.A. Dobrovolskaia, Endocrinology 151 (2010) 458–465.
[206] A.S. Cordeiro, Y. Patil-Sen, M. Shivkumar, R. Patel, A. Khedr, M.A. Elsawy, Pharmaceutics 13 (2021).
[207] A.S. Cordeiro, Y. Farsakoglu, J. Crecente-Campo, M. de la Fuente, S.F. González, M.J. Alonso, Drug Deliv. Transl. Res. 11 (2021) 1689–1702.
[208] A.S. Cordeiro, M.J. Alonso, Pharmaceut. Patent Analyst 5 (2015) 49–73.
[209] A.S. Cordeiro, M.J. Alonso, M. de la Fuente, Biotechnol. Adv. 33 (2015) 1279–1293.
[210] A. Hajizade, F. Ebrahimi, A.-H. Salmanian, A. Arpanaei, J. Amani, J. Appl. Biotechnol. Rep. 1 (2014) 125–134.
[211] S. Hamdy, P. Elamanchili, A. Alshamsan, O. Molavi, T. Satou, J. Samuel, J. Biomed. Mater. Res., Part A 81 (2007) 652–662.
[212] S. Hamdy, O. Molavi, Z. Ma, A. Haddadi, A. Alshamsan, Z. Gobti, S. Elhasi, J. Samuel, A. Lavasanifar, Vaccine 26 (2008) 5046–5057.
[213] X. Hong, X. Zhong, G. Du, Y. Hou, Y. Zhang, Z. Zhang, T. Gong, L. Zhang, X. Sun, Sci. Adv. 6 (2020) eaaz4462.
[214] A.S. Cordeiro, J. Crecente-Campo, B.L. Bouzo, S.F. González, M. de la Fuente, M.J. Alonso, J. Drug Target. 27 (2019) 646–658.
[215] D.A. Rao, M.L. Forrest, A.W. Alani, G.S. Kwon, J.R. Robinson, J. Pharmaceut. Sci. 99 (2010) 2018–2031.
[216] M.A. Swartz, Adv. Drug Deliv. Rev. 50 (2001) 3–20.
[217] S. Kang, S. Ahn, J. Lee, J.Y. Kim, M. Choi, V. Gujrati, H. Kim, J. Kim, E.-C. Shin, S. Jon, J. Contr. Release 256 (2017) 56–67.
[218] Q.H. Quach, S.K. Ang, J.-H.J. Chu, J.C.Y. Kah, Acta Biomater. 78 (2018) 224–235.
[219] B.G. Cha, J.H. Jeong, J. Kim, ACS Cent. Sci. 4 (2018) 484–492.
[220] M. Jambhrunkar, Y. Yang, M. Yu, M. Zhang, P. Abbaraju, T. Ghosh, M. Kalantari, Y. Wang, N. McMillan, C. Yu, Mater. Today Adv. 6 (2020), 100069.
[221] J.Y. Lee, M.K. Kim, T.L. Nguyen, J. Kim, ACS Appl. Mater. Interfaces 12 (2020) 34658–34666.
[222] P.L. Abbaraju, A.K. Meka, H. Song, Y. Yang, M. Jambhrunkar, J. Zhang, C. Xu, M. Yu, C. Yu, J. Am. Chem. Soc. 139 (2017) 6321–6328.
[223] B. Sun, Z. Ji, Y.-P. Liao, M. Wang, X. Wang, J. Dong, C.H. Chang, R. Li, H. Zhang, A.E. Nel, ACS Nano 7 (2013) 10834–10849.
[224] S. Zanganeh, G. Hutter, R. Spitler, O. Lenkov, M. Mahmoudi, A. Shaw, J.S. Pajarinen, H. Nejadnik, S. Goodman, M. Moseley, Nat. Nanotechnol. 11 (2016) 986–994.
[225] C. Nathan, A. Cunningham-Bussel, Nat. Rev. Immunol. 13 (2013) 349–361.
[226] T.-C. Cheong, E.P. Shin, E.-K. Kwon, J.-H. Choi, K.-K. Wang, P. Sharma, K.H. Choi, J.-M. Lim, H.-G. Kim, K. Oh, ACS Chem. Biol. 10 (2015) 757–765.
[227] C. Wang, P. Li, L. Liu, H. Pan, H. Li, L. Cai, Y. Ma, Biomaterials 79 (2016) 88–100.
[228] L. Galluzzi, L. Senovilla, L. Zitvogel, G. Kroemer, Nat. Rev. Drug Discov. 11 (2012) 215–233.
[229] C. Pfirschke, C. Engblom, S. Rickelt, V. Cortez-Retamozo, C. Garris, F. Pucci, T. Yamazaki, V. Poirier-Colame, A. Newton, Y. Redouane, Immunity 44 (2016) 343–354.
[230] A. Haque, N.L. Banik, S.K. Ray, Neurochem. Res. 32 (2007) 2203–2209.
[231] D.I. Gabrilovich, S. Nagaraj, Nat. Rev. Immunol. 9 (2009) 162–174.
[232] T. Whiteside, Oncogene 27 (2008) 5904–5912.

[233] D.M. Pardoll, Nat. Med. 4 (1998) 525–531.
[234] P. Cresswell, A.L. Ackerman, A. Giodini, D.R. Peaper, P.A. Wearsch, Immunol. Rev. 207 (2005) 145–157.
[235] H.T. Idriss, J.H. Naismith, Microsc. Res. Tech. 50 (2000) 184–195.
[236] A. Montfort, C. Colacios, T. Levade, N. Andrieu-Abadie, N. Meyer, B. Ségui, Front. Immunol. 10 (2019).
[237] J. Wagner, D. Gößl, N. Ustyanovska, M. Xiong, D. Hauser, O. Zhuzhgova, S. Hočevar, B. Taskoparan, L. Poller, S. Datz, H. Engelke, Y. Daali, T. Bein, C. Bourquin, ACS Nano 15 (2021) 4450–4466.
[238] D. Kwon, B.G. Cha, Y. Cho, J. Min, E.-B. Park, S.-J. Kang, J. Kim, Nano Lett. 17 (2017) 2747–2756.
[239] F. Wu, T. Xu, G. Zhao, S. Meng, M. Wan, B. Chi, C. Mao, J. Shen, Langmuir : ACS J. Surf. Collids 33 (2017).
[240] L. Chen, X. Ma, M. Dang, H. Dong, H. Hu, X. Su, W. Liu, Q. Wang, Y. Mou, Z. Teng, Adv. Healthc. Mater. 8 (2019), 1900039.
[241] Q.U. Ain, E.V.R. Campos, A. Huynh, D. Witzigmann, S. Hedtrich, Trends Biotechnol. 39 (2021) 474–487.
[242] D.P. Feldmann, J. Heyza, C.M. Zimmermann, S.M. Patrick, O.M. Merkel, Molecules 25 (2020).
[243] A. Mehta, T. Michler, O.M. Merkel, Adv. Healthc. Mater. 10 (2021), 2001650.
[244] G. Dorraj, J.J. Carreras, H. Nunez, I. Abushammala, A. Melero, Curr. Gene Ther. 17 (2017) 89–104.
[245] X. Du, B. Shi, J. Liang, J. Bi, S. Dai, S.Z. Qiao, Adv. Mater. 25 (2013) 5981–5985.
[246] Y. Wang, H. Song, M. Yu, C. Xu, Y. Liu, J. Tang, Y. Yang, C. Yu, J. Mater. Chem. B 6 (2018) 4089–4095.
[247] T. Yu, X. Liu, A.L. Bolcato-Bellemin, Y. Wang, C. Liu, P. Erbacher, F. Qu, P. Rocchi, J.P. Behr, L. Peng, Angew. Chem. Int. Ed. 51 (2012) 8478–8484.
[248] G. Yu, X. Zhao, J. Zhou, Z. Mao, X. Huang, Z. Wang, B. Hua, Y. Liu, F. Zhang, Z. He, J. Am. Chem. Soc. 140 (2018) 8005–8019.
[249] T.T. Hoang, T.P. Smith, R.T. Raines, Angew. Chem. 129 (2017) 2663–2666.
[250] J. Li, K. Pu, Chem. Soc. Rev. 48 (2019) 38–71.
[251] H. Li, H. Guo, C. Lei, L. Liu, L. Xu, Y. Feng, J. Ke, W. Fang, H. Song, C. Xu, C. Yu, X. Long, Adv. Mater. 31 (2019), 1904535.
[252] Y. Chen, H. Chen, J. Shi, Adv. Mater. 25 (2013) 3144–3176.
[253] J.G. Croissant, Y. Fatieiev, A. Almalik, N.M. Khashab, Adv. Healthc. Mater., 7, 2018, 1700831.
[254] L. Chen, X. Zhou, C. He, Wiley Interdiscip. Rev. Nanomed. Nanotechnol. 11 (2019) e1573.
[255] C. Lei, Y. Cao, S. Hosseinpour, F. Gao, J. Liu, J. Fu, R. Staples, S. Ivanovski, C. Xu, Nano Res. 14 (2021) 770–777.
[256] C.-T. Kao, Y.-J. Chen, T.-H. Huang, Y.-H. Lin, T.-T. Hsu, C.-C. Ho, Processes 8 (2020).
[257] M. Mehrasa, M.A. Asadollahi, K. Ghaedi, H. Salehi, A. Arpanaei, Int. J. Biol. Macromol. 79 (2015) 687–695.
[258] M. Mehrasa, M.A. Asadollahi, B. Nasri-Nasrabadi, K. Ghaedi, H. Salehi, A. Dolatshahi-Pirouz, A. Arpanaei, Mater. Sci. Eng. C Mater. Biol. Appl. 66 (2016) 25–32.
[259] Y. Li, Y. Guo, J. Ge, P.X. Ma, B. Lei, Appl. Mater. Today 10 (2018) 153–163.
[260] B. Baumann, T. Jungst, S. Stichler, S. Feineis, O. Wiltschka, M. Kuhlmann, M. Lindén, J. Groll, Angew. Chem. Int. Ed. 56 (2017) 4623–4628.
[261] N. Wang, M. Ma, Y. Luo, T. Liu, P. Zhou, S. Qi, Y. Xu, H. Chen, ChemNanoMat 4 (2018) 631–641.
[262] S. Yang, J. Wang, H. Tan, F. Zeng, C. Liu, Soft Matter 8 (2012) 8981–8989.
[263] S. Rose, A. Prevoteau, P. Elzière, D. Hourdet, A. Marcellan, L. Leibler, Nature 505 (2014) 382–385.
[264] A. Pamukcu, D. Sen Karaman, EVALUATION OF DENDRITIC MESOPOROUS SILICA NANOPARTICLES FOR AMENDING THE CELL VIABILITY IN THREE-DIMENSIONAL CELL CULTURE MATRIX, 2021.
[265] X. Guo, J. Zhu, H. Zhang, Z. You, Y. Morsi, X. Mo, T. Zhu, J. Colloid Interface Sci. 539 (2019) 351–360.
[266] H. Kuang, Y. Wang, J. Hu, C. Wang, S. Lu, X. Mo, ACS Appl. Mater. Interfaces 10 (2018) 19365–19372.
[267] R.S. de Oliveira, S.S. Fantaus, A.J. Guillot, A. Melero, R.C. Beck, Pharmaceutics 13 (2021).
[268] S. Obuobi, Z.X. Voo, M.W. Low, B. Czarny, V. Selvarajan, N.L. Ibrahim, Y.Y. Yang, P.L.R. Ee, Adv. Healthc. Mater. 7 (2018), 1701388.
[269] J. Wang, V. Planz, B. Vukosavljevic, M. Windbergs, Eur. J. Pharm. Biopharm. 129 (2018) 175–183.
[270] H. Wu, F. Li, S. Wang, J. Lu, J. Li, Y. Du, X. Sun, X. Chen, J. Gao, D. Ling, Biomaterials 151 (2018) 66–77.
[271] Z. Pan, K.-R. Zhang, H.-L. Gao, Y. Zhou, B.-B. Yan, C. Yang, Z.-y. Zhang, L. Dong, S.-M. Chen, R. Xu, D.-H. Zou, S.-H. Yu, Nano Res. 13 (2020) 373–379.
[272] M. Shi, Y. Zhou, J. Shao, Z. Chen, B. Song, J. Chang, C. Wu, Y. Xiao, Acta Biomater. 21 (2015) 178–189.
[273] V. Selvarajan, S. Obuobi, P.L.R. Ee, Front. Chem. 8 (2020) 602.
[274] C.R. Thorn, N. Thomas, B.J. Boyd, C.A. Prestidge, Drug Deliv. Transl. Res. 11 (2021) 1598–1624.
[275] C.R. Thorn, P.L. Howell, D.J. Wozniak, C.A. Prestidge, N. Thomas, Adv. Drug Deliv. Rev. 179 (2021), 113916.
[276] Y. Wang, Y. Wang, X. Li, J. Li, L. Su, X. Zhang, X. Du, ACS Sustain. Chem. Eng. 6 (2018) 14071–14081.
[277] Y. Wang, Y.A. Nor, H. Song, Y. Yang, C. Xu, M. Yu, C. Yu, J. Mater. Chem. B 4 (2016) 2646–2653.
[278] Y. Wang, Y. Wang, L. Su, Y. Luan, X. Du, X. Zhang, J. Alloys Compd. 783 (2019) 136–144.
[279] B. Beitzinger, F. Gerbl, T. Vomhof, R. Schmid, R. Noschka, A. Rodríguez, S. Wiese, G. Weidinger, L. Staendker, P. Walther, J. Michaelis, M. Lindén, S. Stenger, Adv. Healthc. Mater. 10 (2021), 2100453.
[280] Y. Zhang, Q. Zhang, F. Wei, N. Liu, OncoTargets Ther. 12 (2019) 5457–5465.
[281] C. Mo, L. Lu, D. Liu, K. Wei, J. Nanobiotechnol. 18 (2020) 55.
[282] Y. Yu, Z. Wang, Q. Yang, Q. Ding, R. Wang, Z. Li, Y. Fang, J. Liao, W. Qi, K. Chen, M. Li, Y.Z. Zhu, Drug Deliv. 28 (2021) 1031–1042.
[283] F. Tang, L. Li, D. Chen, Adv. Mater. 24 (2012) 1504–1534.
[284] X. Wang, X. Li, A. Ito, K. Yoshiyuki, Y. Sogo, Y. Watanabe, A. Yamazaki, T. Ohno, N.M. Tsuji, Small 12 (2016) 3510–3515.
[285] Y. Chen, P. Xu, H. Chen, Y. Li, W. Bu, Z. Shu, Y. Li, J. Zhang, L. Zhang, L. Pan, Adv. Mater. 25 (2013) 3100–3105.
[286] X. Chen, M. Chen, Theranostics 10 (2020) 7403.
[287] A.B.E. Attia, G. Balasundaram, M. Moothanchery, U.S. Dinish, R. Bi, V. Ntziachristos, M. Olivo, Photoacoustics 16 (2019), 100144.
[288] H. Xiong, S. Du, J. Ni, J. Zhou, J. Yao, Biomaterials 94 (2016) 70–83.
[289] X. Wang, X. Li, A. Ito, Y. Sogo, Y. Watanabe, K. Hashimoto, A. Yamazaki, T. Ohno, N.M. Tsuji, Chem. Commun. 54 (2018) 1057–1060.